[redacted]

[redacted]

LTV
ASTRONAUTICS DIVISION
CHANCE VOUGHT CORP
A DIVISION OF LING-TEMCO-VOUGHT, INC.
POST OFFICE BOX 6267 DALLAS 22, TEXAS

(NASA-CR-142167) SPACE SUIT THERMAL TEST PROGRAM Final Report (Chance Vought Corp.) 71 p

N75-71942

Unclas

Report No. 00.79

Dated: 2 September 1962

FINAL REPORT

"SPACE SUIT THERMAL TEST PROGRAM" (u)

CONTRACT NAS 9-461

2 SEPTEMBER 1962

SUBMITTED BY
ASTRONAUTICS DIVISION
CHANCE VOUGHT CORPORATION
P. O. Box 6267 . Dallas 22, Texas

TO

NATIONAL AERONAUTICS AND SPACE ADMINISTRATION

Prepared by:

R. A. Knezek
Power & Environment

R. J. French
Power & Environment

Approved by:

G. B. Whisenhunt
Power & Environment

M. H. Bradshaw
Manager, R&D Programs

[redacted]

10134

ABSTRACT

A test program was conducted in a simulated space environment to determine the feasibility and effectiveness of an insulated coverall garment in providing thermal control of extra-vehicular space suits. The test articles consisted of a Project Mercury full-pressure suit, a coverall garment, and a dummy man.

The results of the program indicated that the use of a coverall garment is feasible and effective. This is shown by the small influence of varying environmental conditions on the temperature at the inner surfaces of the coverall and pressure suit and by the low heat losses through the coverall to a cold space environment. Significant deterioration of the coverall and pressure suit visor materials occurred during the tests. Future work should include analysis and element testing to determine the most suitable materials and insulation thicknesses followed by comprehensive full scale testing of the improved coverall garment.

[redacted]

[redacted]

TABLE OF CONTENTS

[redacted]

[redacted]

LIST OF FIGURES

[redacted]

LIST OF TABLES

[redacted]

1.0 INTRODUCTION

Manned Space programs have indicated that man will be required to perform functions outside the protective enclosure of his sealed spacecraft. These functions will include repairs to the outside of the vehicle, transfer from one vehicle to another, assembly of space stations, and exploration of the lunar surface. During these operations, the astronaut will be exposed to the extremes of the space environment. In some instances, he will be on the sunlit side of the vehicle or the moon where he will receive heat in the form of radiation from the sun, vehicle, earth, and moon. He will also be required to perform tasks on the shaded side of a vehicle where he will be subjected to the extreme cold of space and will receive only a small amount of thermal radiation. Current full-pressure suits will not adequately protect the space worker from these extremes of thermal environment.

Preliminary analyses have indicated that adequate thermal protection for extra-vehicular operation could be obtained by use of an insulated coverall garment worn over a normal vehicular pressure suit. This approach is possible because of the extremely low thermal conductivities exhibited by low density superinsulations under vacuum conditions. The coverall garment will reduce heat inputs and heat losses from the pressure suit sufficiently to allow adequate thermal control of the suit interior by an air circulation and conditioning system. Since the air circulation and conditioning system is required for pressurization and breathing gas, no complicated equipment must be added to accomplish the extra-vehicular thermal control function.

In order to investigate the above extra-vehicular space suit thermal control concept by actual tests, an insulated coverall garment was fabricated by the National Aeronautics and Space Administration Manned Spacecraft Center, Houston, Texas. Under NASA contract No. NAS 9-461, Vought Astronautics Division, Ling-Temco-Vought, Inc., conducted tests in a simulated space environment to determine the feasibility of the insulated coverall concept for thermal protection in space and to determine the thermal effectiveness of the coverall. This report summarizes the results of this test program.

[redacted]

2.0 SUMMARY

A test program was conducted in a simulated space environment to determine the feasibility and effectiveness of an insulated coverall garment as a method for extra-vehicular space suit thermal control. The test articles used during the program included a project Mercury full pressure suit assembly, an anthropometric dummy, and an insulated coverall garment. The pressure suit and the insulated coverall garment were supplied by the NASA Manned Spacecraft Center. Thermal tests were conducted with the dummy clothed in both the coverall garment and pressure suit and with the dummy clothed in the pressure suit only. The space environmental conditions simulated during the test program included vacuum, coldness of deep space, and solar heating.

The test results show that the insulated coverall concept is feasible and is an effective method for thermal control of an extra-vehicular space suit. With the coverall in place, the temperature of the inner surface of the pressure suit remained within limits that would be comfortable for a man. The heat losses through the coverall in the cold environment (no solar heating) were determined to be between 3 and 10 BTU/hr ft^2.

A significant detrimental effect encountered during the test program was deterioration of materials exposed to the space environment. The outer surface of the coverall (aluminized mylar with the mylar exposed) had deteriorated badly after three days of testing. This layer was very fragile and was badly torn. The pressure suit helmet visor and visor shield also showed signs of deterioration. Deformation and irregularities in the visor and visor shield surfaces were observed. This significant deterioration of the coverall and the visor impose the requirement for additional study to determine materials for the external surfaces which will withstand the extremes of the space environment.

Analysis and element testing should be conducted to select the most suitable outer surface materials and insulation thickness. When these parameters are established, a complete coverall garment incorporating the best features from the element tests should be constructed and comprehensive full scale tests conducted. This procedure will provide a suitable coverall garment within the schedule requirements of current manned space programs.

[redacted]

3.0 TEST PROGRAM

3.1 Objective

The objective of this program was to determine the feasibility and effectiveness of the insulated coverall garment concept for extra-vehicular space suit thermal control. This was accomplished by thermally testing the coverall in a simulated space environment. The coveralls were installed over a Project Mercury type full pressure suit through which air was circulated. A dummy man was used to obtain air flow rates and distribution similar to that which an actual man would experience. The dummy, however, did not simulate the heat capacity of the man or his heat dissipation.

Originally, it was anticipated that one-half hour or less would be required to obtain stable test conditions and a test program to investigate a large number of test points was planned. These test points included various air flow rates, suit pressures, orientations, and air temperatures. After the first day of testing, however, it was found that the temperatures of the test article required a much longer time to stabilize due to the effectiveness of the coverall garment. The NASA Technical Monitor and the contractor concurred that the objectives of the program could be accomplished more effectively by reducing the number of test points and allowing the temperatures to stabilize for a longer period of time. The revised test program which was conducted is described in the following paragraphs

3.2 Test Articles

The three basic test articles for this program consisted of an anthropometric dummy man, a full pressure suit assembly, and an insulated coverall garment. The dummy was manufactured by Sierra Engineering Company, Sierra Madre, California. It had the dimensions of a 5th percentile man, Reference 1, and weighed 53 pounds. The inner bulk of the dummy was molded foam rubber with approximately 1/4 inch of vinyl rubber providing a tough outer surface. An aluminum framework with steel joints in the flexure regions provided support for the flexible rubber. The steel joints at the knees and hips were tightened so the dummy would stand erect in the test facility with minimum external supports. Figure 1 shows a photograph of the dummy with the instrumentation installed.

The pressure suit was a well worn Project Mercury suit. Because of the previous use, much of the original bright aluminized surface had been worn away exposing the dull green fabric. Relatively new shoes and gloves were supplied with the suit. The shoes had a bright aluminized surface and the gloves were green with black leather segments. The pressure suit is shown in Figure 2 with the coverall partially installed.

The pressure suit helmet, which is normally equipped with a clear visor, also had attachments for a visor shield. The visor

[redacted]

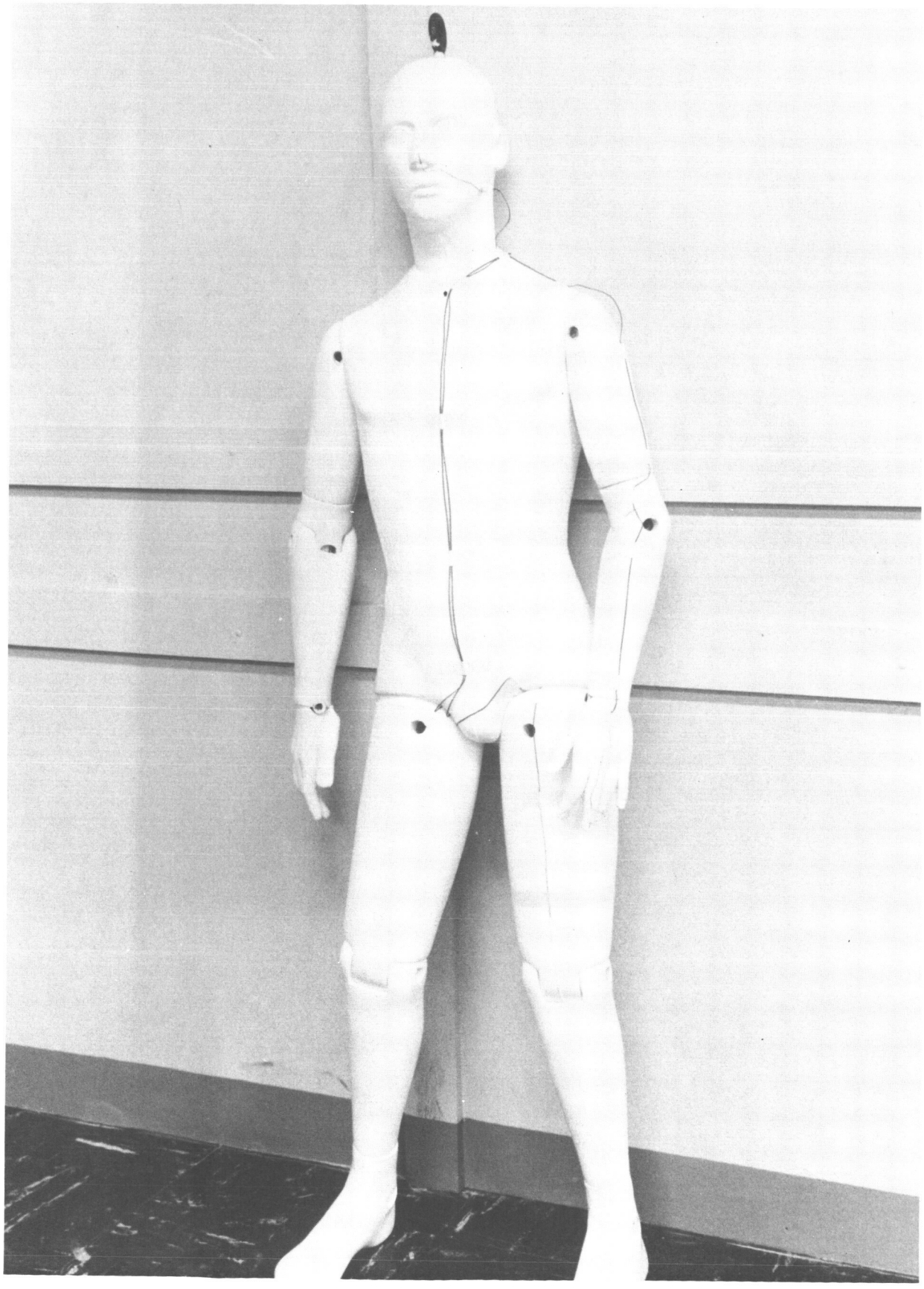

Figure 1 ANTHROPOMETRIC DUMMY

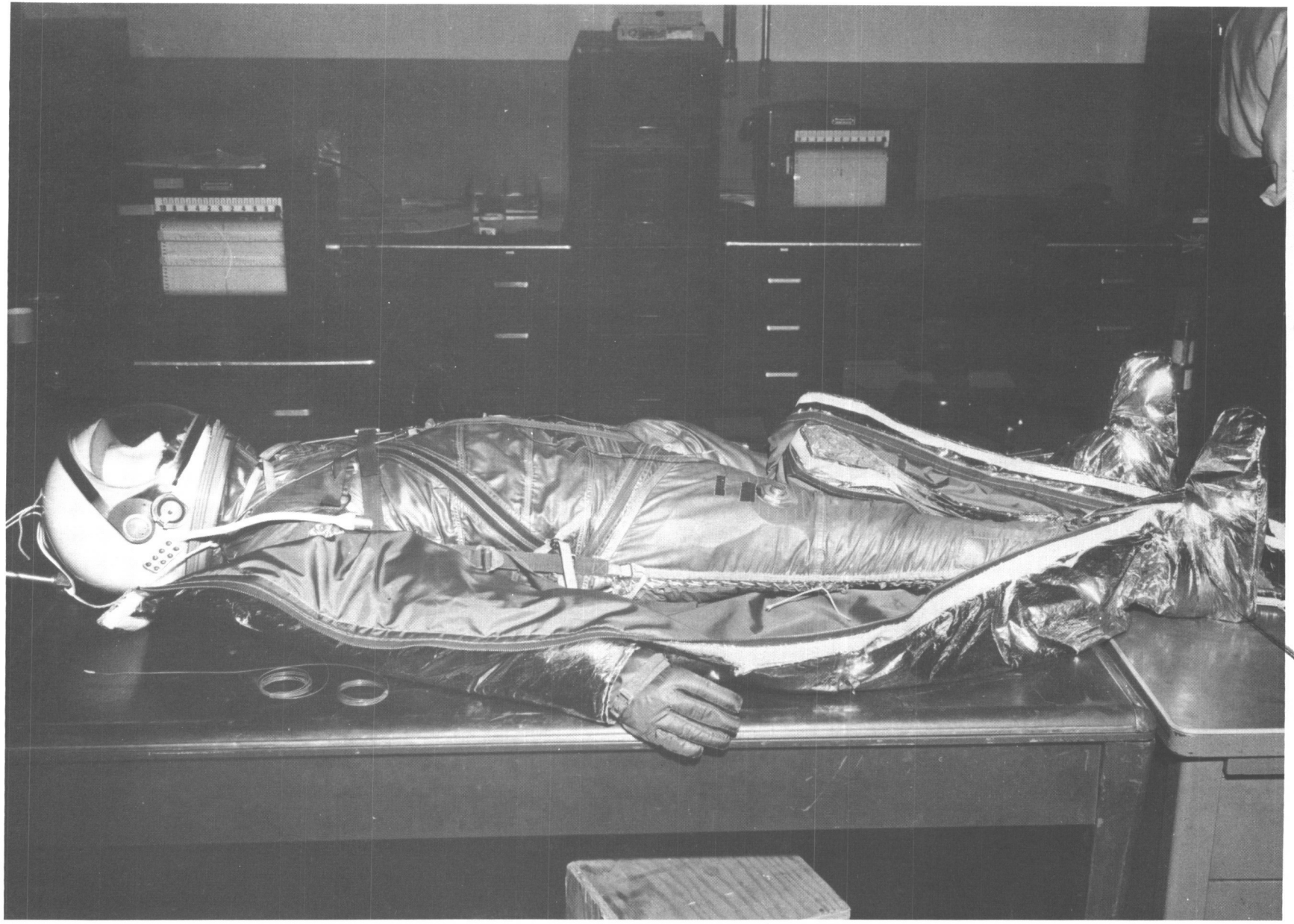

Figure 2 PRESSURE SUIT AND COVERALL INSTALLATION

[redacted] shield was made of plastic and was coated with a thin transparent gold film on the outer surface. Thermal tests of the pressure suit and coverall assembly were made with and without the visor shield in place.

The insulated coverall was fabricated by the NASA Manned Spacecraft Center from National Research Corporation multi-layer super insulation. This insulation consisted of 25 layers of aluminized mylar separated by thin layers of dacron felt. Chafing of the inner surface of the insulation was prevented by a fabric sewed in as an integral part of the coverall. The total insulation thickness was approximately 1/4 inch. Construction of the coverall material is shown in Figure 3.

The coverall was a one-piece garment with the exception of the helmet cover and the hand mittens. Zipper seams at the front of the coverall provided openings for donning. Venting of the insulation to the vacuum chamber was provided by seam leakage and by openings where the hand mittens and helmet cover were attached to the main coverall. Areas of the coverall that could have trapped air were vented by perforating with a sewing machine needle. The needle holes allowed the air to escape from the inner layers of material. The test article installation is shown in Figure 4.

3.3 Test Equipment

3.3.1 Space Environment Simulator

The Chance Vought Space Environment Simulator was used to simulate the space conditions of high vacuum, extreme cold, and solar radiation. An overall view of the simulator is shown in Figure 5. A chamber pressure of 7×10^{-5} to 9×10^{-5} mm of Hg was maintained throughout the tests by three stages of pumping. The pumping system includes three oil diffusion pumps, an oil ejector pump, and a mechanical ballast pump.

The cold of deep space was simulated by liquid nitrogen cooled walls with a high emissivity. A cold wall temperature of $-310^{\circ}F$ was maintained throughout the test program.

Solar simulation was provided by a bank of Mercury-Xenon high pressure DC arc lamps. The solar heat flux at the target test plane was calibrated before and after the test program. Lamp wattages were also monitored during the tests to determine any fluctuations in the heat flux. Figure 6 shows a typical heat flux obtained during the test. The heat flux at the target plane had a nominal $\pm 10\%$ variation from the desired flux of 440 BTU/hr ft^2. A survey of test data shows occasionally 2 or 3 lamps varied more, but not further than 15% from the desired 440 BTU/hr ft^2.

The spectral energy distribution of the solar source is shown in Table 1. This distribution was determined by use of bandpass filters and thermopiles in survey of the energy distribution for eleven lamps.

[redacted]

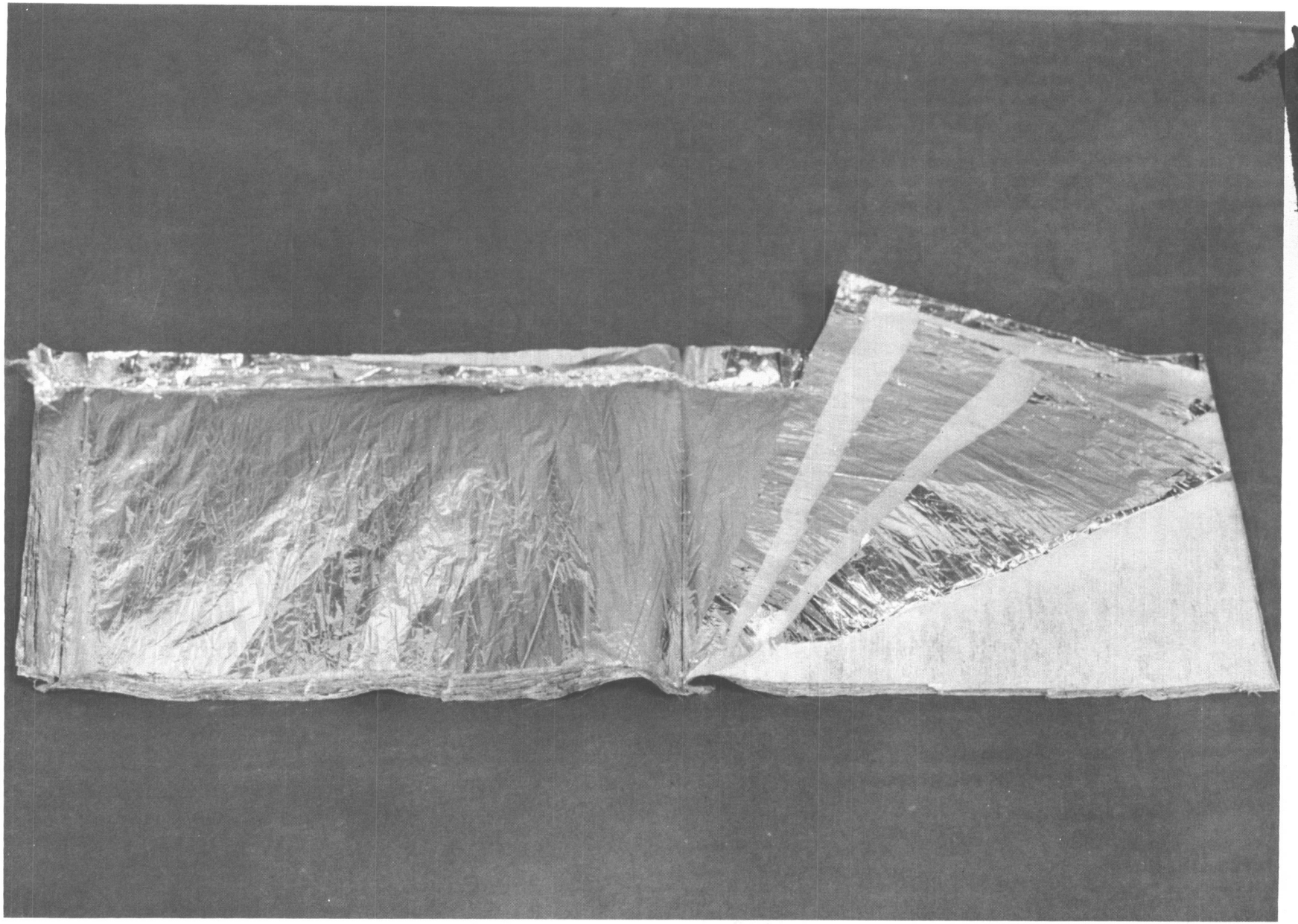

Figure 3 COVERALL MATERIAL CONSTRUCTION

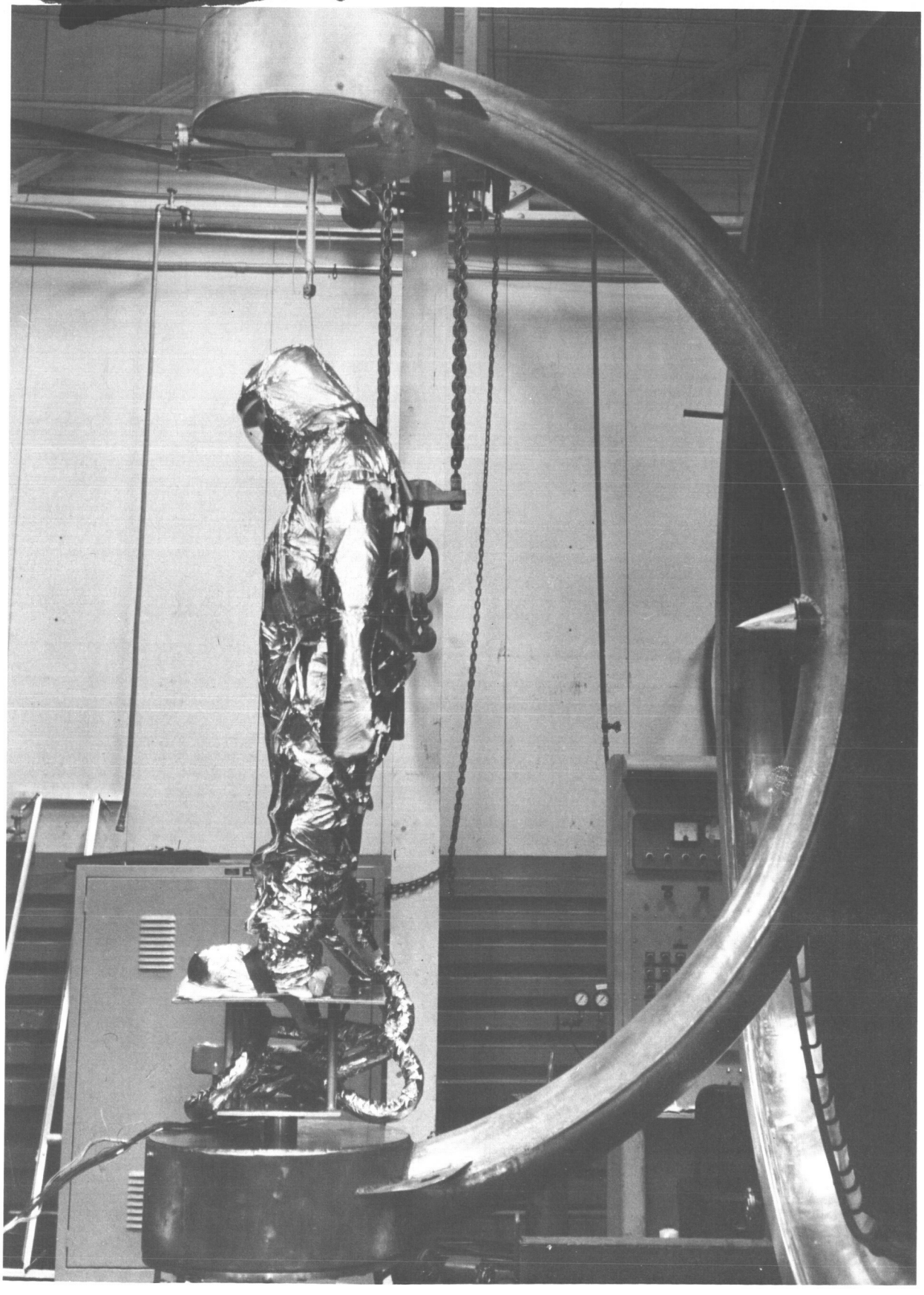

Figure 4 MODEL MOUNTING IN SPACE ENVIRONMENT SIMULATOR

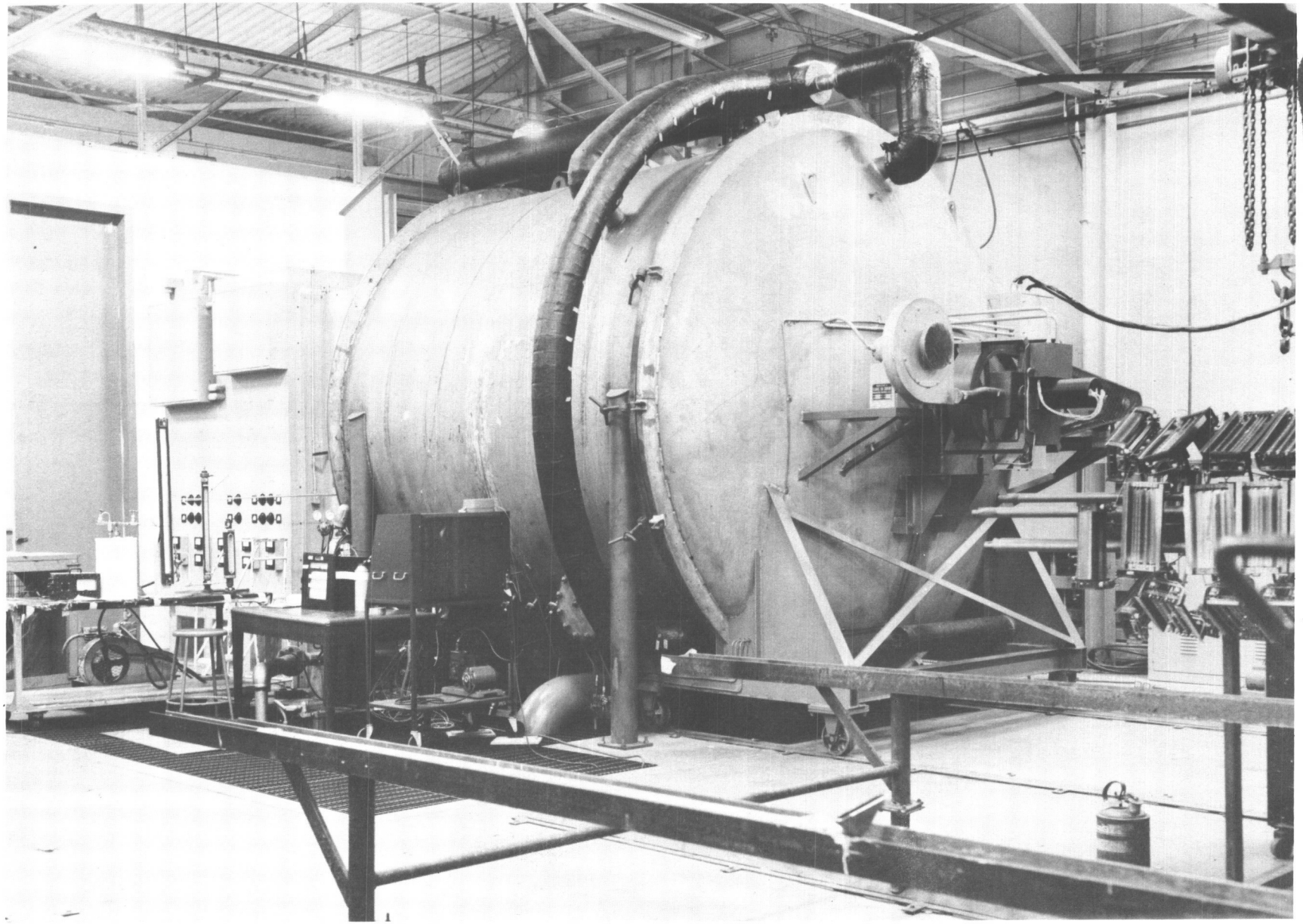

Figure 5 SPACE ENVIRONMENT SIMULATOR

FIGURE 6

TYPICAL SOLAR SOURCE HEAT FLUX DISTRIBUTION
AT TARGET PLANE

DESIRED FLUX = 440 $\frac{BTU}{hr\ ft^2}$

○ Lamp

◌ Pickup

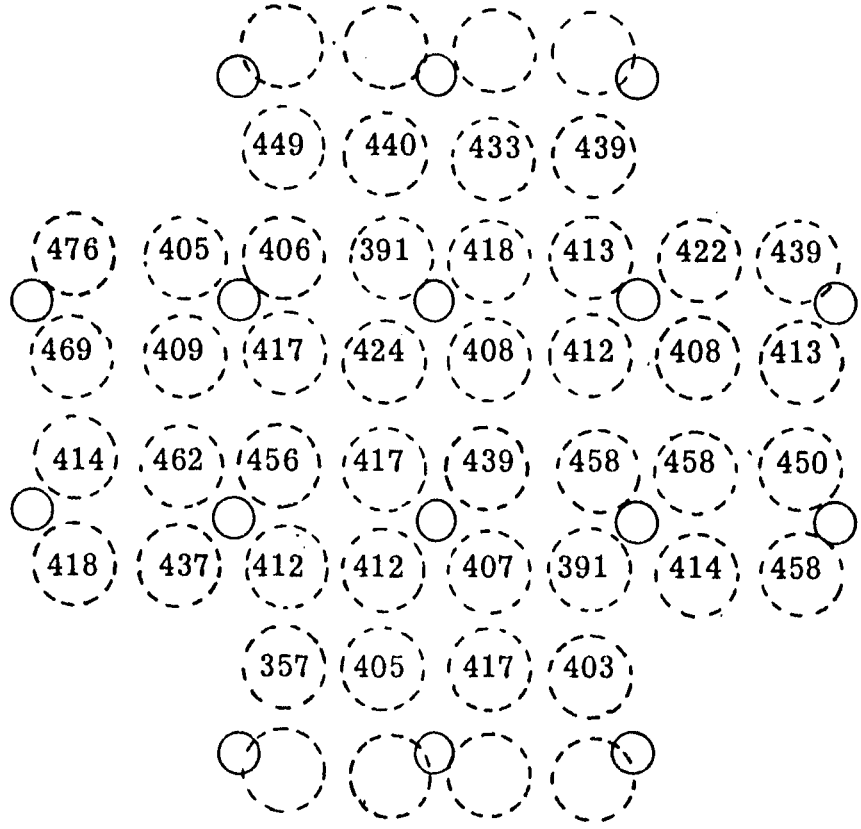

[redacted]

TABLE 1

SPECTRAL ENERGY DISTRIBUTION

Wavelength λ (mμ)	Energy mw cm^{-2}	Wavelength λ (mμ)	Energy mw cm^{-2}
260	(0.5)	560- 70	0.2
260- 70	1.0	70- 80	2.7
70- 80	1.5	80- 90	2.2
80- 90	1.7	590-600	0.2
290-300	2.0	600- 10	0.1
300- 10	2.5	10- 20	0.6
10- 20	2.6	20- 30	0.1
20- 30	0.4	30- 40	0.1
30- 40	1.2	40- 50	0.1
40- 50	0.2	50- 60	0.1
50- 60	0.4	60- 70	0.1
60- 70	3.6	70- 80	1.1
70- 80	0.5	80- 90	0.4
80- 90	0.3	690-700	0.1
390-400	0.2	700-750	0.5
400- 10	1.7	750-800	0.4
10- 20	0.2	800-850	0.7
20- 30	0.3	850-900	1.0
30- 40	3.4	900-950	0.9
40- 50	0.2	950-1000	1.0
50- 60	0.2	1000-1100	2.0
60- 70	0.1	1100-1200	1.8
70- 80	0.1	1200-1300	0.9
80- 90	0.1	1300-1400	1.9
490-500	0.2	1400-1500	0.4
500- 10	0.1	1500-1600	0.5
10- 20	0.1	1600-1700	0.5
20- 30	0.1	1700-1800	0.5
30- 40	0.2	1800-1900	0.2
40- 50	2.5	1900-2000	0.1
550- 60			

[redacted]

[redacted]

3.3.2 Air Flow Equipment

The air flow equipment was designed to provide flow through the pressure suit at the desired temperature, pressure, and flow rate. A schematic of the flow equipment is shown in Figure 7. Air heating was provided by an electrical resistance heater in the air inlet line. Air cooling was provided by an air coil immersed in a bath of methanol which was cooled by dry ice.

Flow through the pressure suit was controlled by the flow control valve in the suit inlet line of the apparatus. Pressure at the outlet of the suit was maintained at the desired level by adjusting the pressure control valve in the outlet line. The pressure drop between pressure suit inlet and outlet was a nominal 0.3 in. of Hg. and varied negligibly throughout the tests. Air was removed from the flow system by a two stage National Research Corporation type 100-C rotary gas ballast pump.

Because of the difficulty in obtaining a dependable pressure relief valve that could be used for the low pressures at which the pressure suit was operated, a mercury blow-out type pressure relief device was constructed. This device is shown schematically in Figure 8. It was designed to relieve should the pressure differential between the pressure suit outlet line and the space chamber exceed 5.75 psia.

3.3.3 Suit Leak Check Equipment

Before installing the pressure suit assembly in the Space Environment Simulator, a leak check of the suit was performed. A schematic of the leak check equipment is shown in Figure 9. The air supply was filtered to remove water and other contaminants. A pressure regulator was used to control the pressure within the suit. During initial pressurization of the suit, the flowmeter was isolated to prevent damage by high flow rates. After the suit pressure had stabilized, the suit pressurization valve was closed and the leakage was measured by the flowmeter. The flowmeter was a type 141-1355 manufactured by Brooks Instrument Company, Hatfield, Penna.

3.4 Instrumentation

3.4.1 Test Article

The test articles were instrumented with 42 copper-constantan thermocouples and two pressure transducers. The instrumentation locations on the test articles are shown in Figures 10 and 11. Tables 2 and 3 summarize the instrumentation read-outs by number and by location. The locations defined by Figure 10 and Table 2 are for tests with the insulated coverall installed over the pressure suit. The locations shown in Figure 11 and Table 3 are for tests without the coverall. During the latter tests, the thermocouples formerly located on the coverall were relocated on the pressure suit.

[redacted]

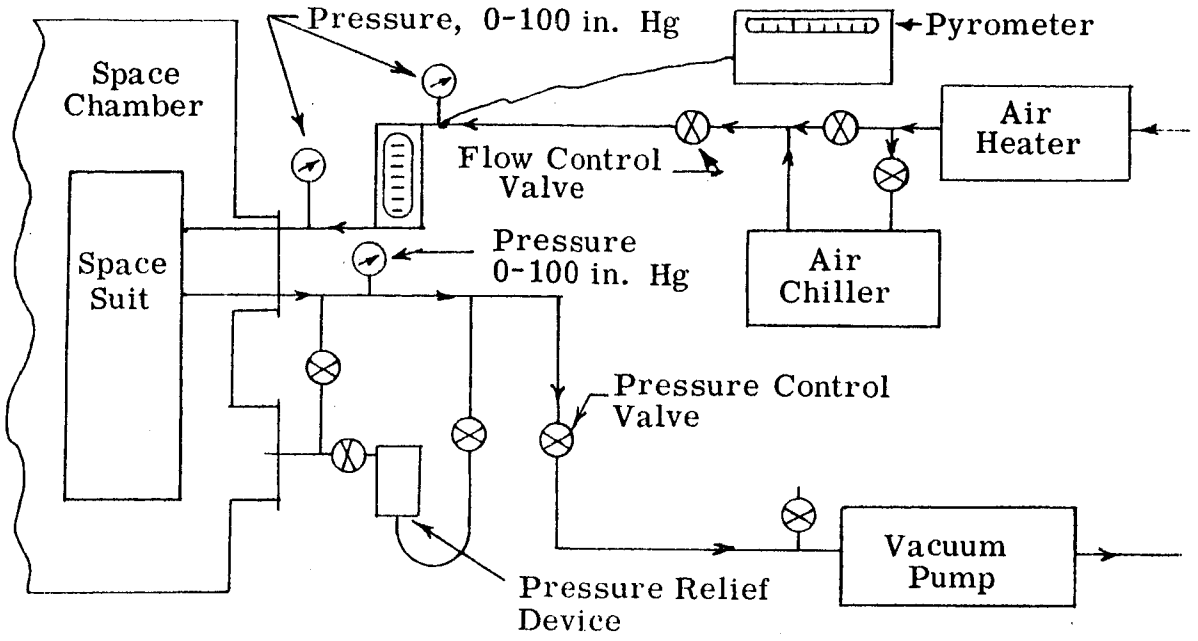

FIGURE 7 SCHEMATIC OF AIR FLOW SYSTEM

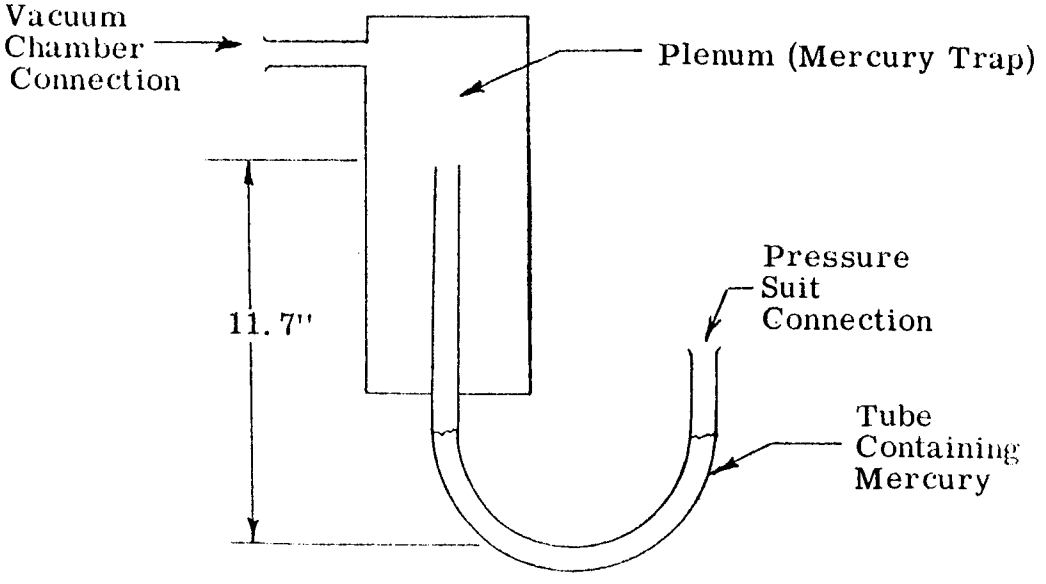

FIGURE 8 SCHEMATIC OF PRESSURE RELIEF DEVICE

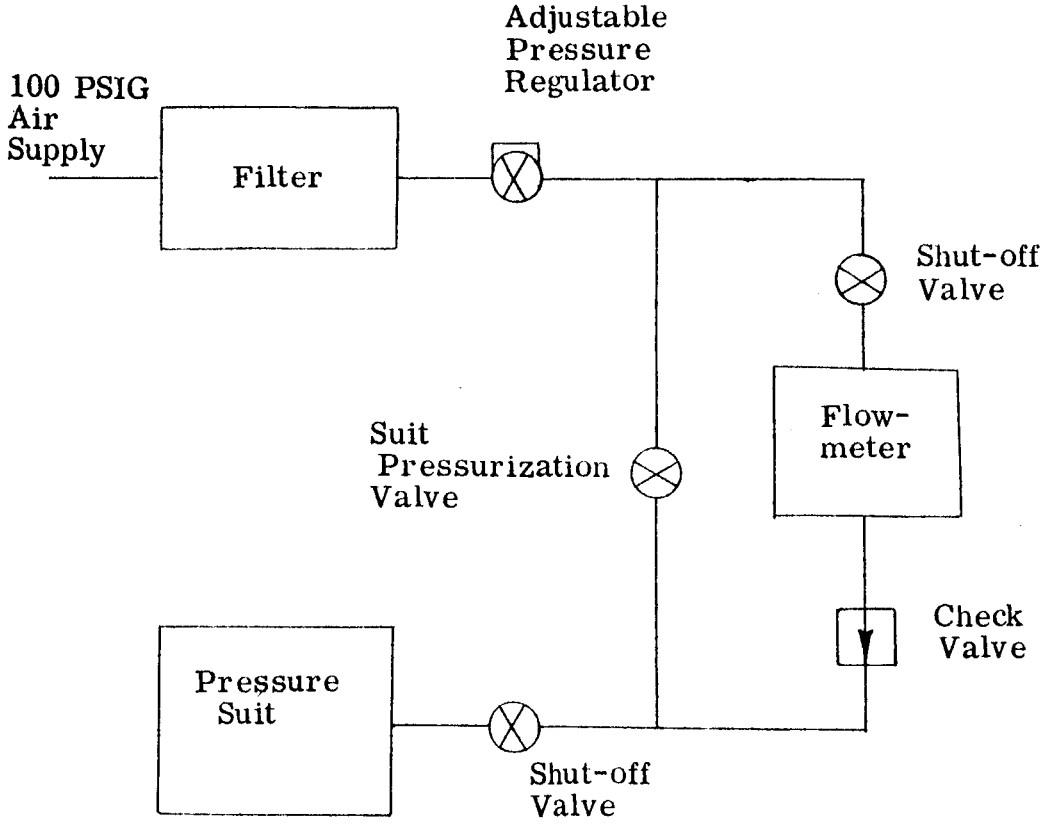

FIGURE 9

SCHEMATIC OF LEAK CHECK EQUIPMENT

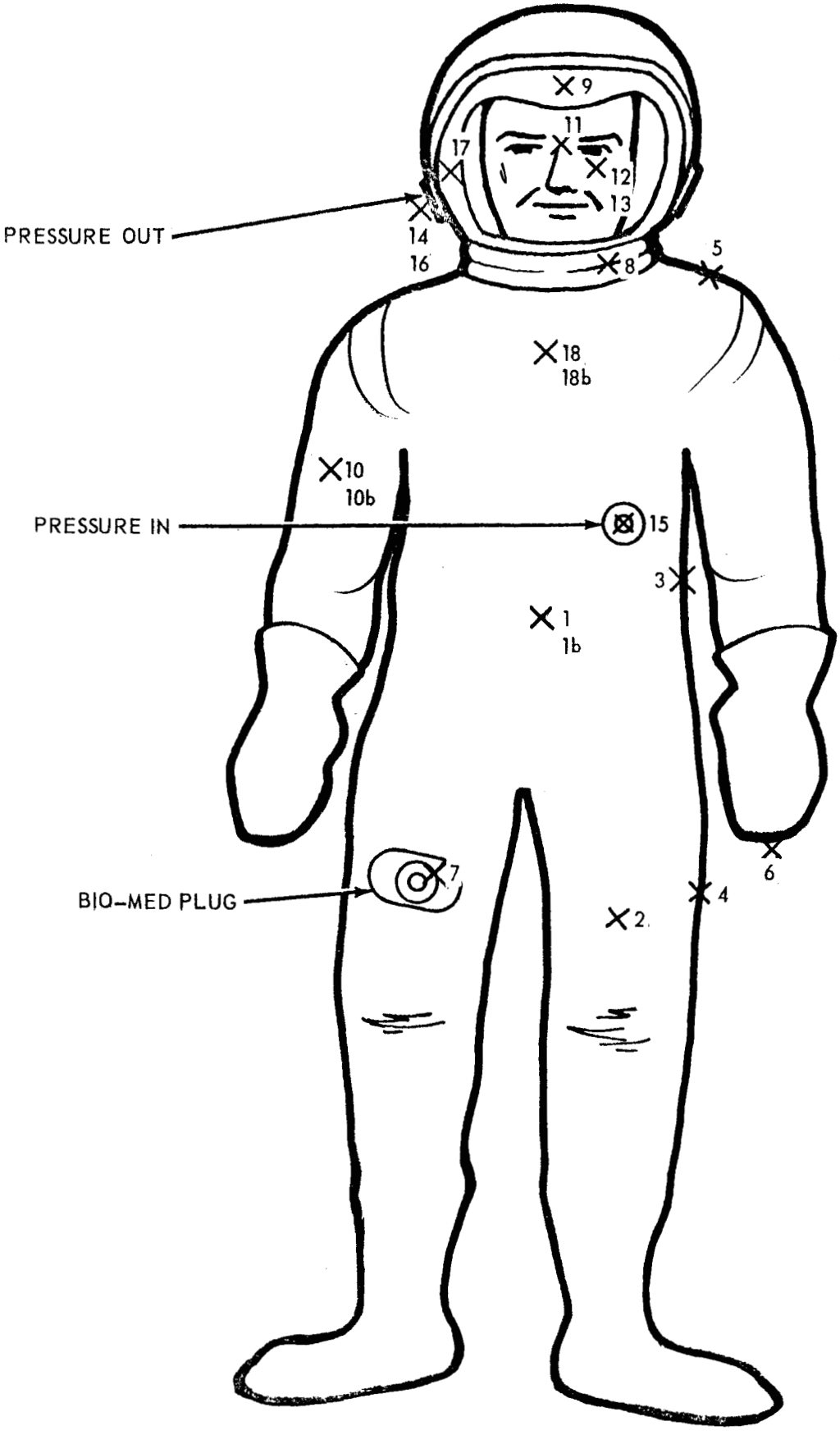

FIGURE 10 INSTRUMENTATION LOCATION , COVERALL ON

[redacted]

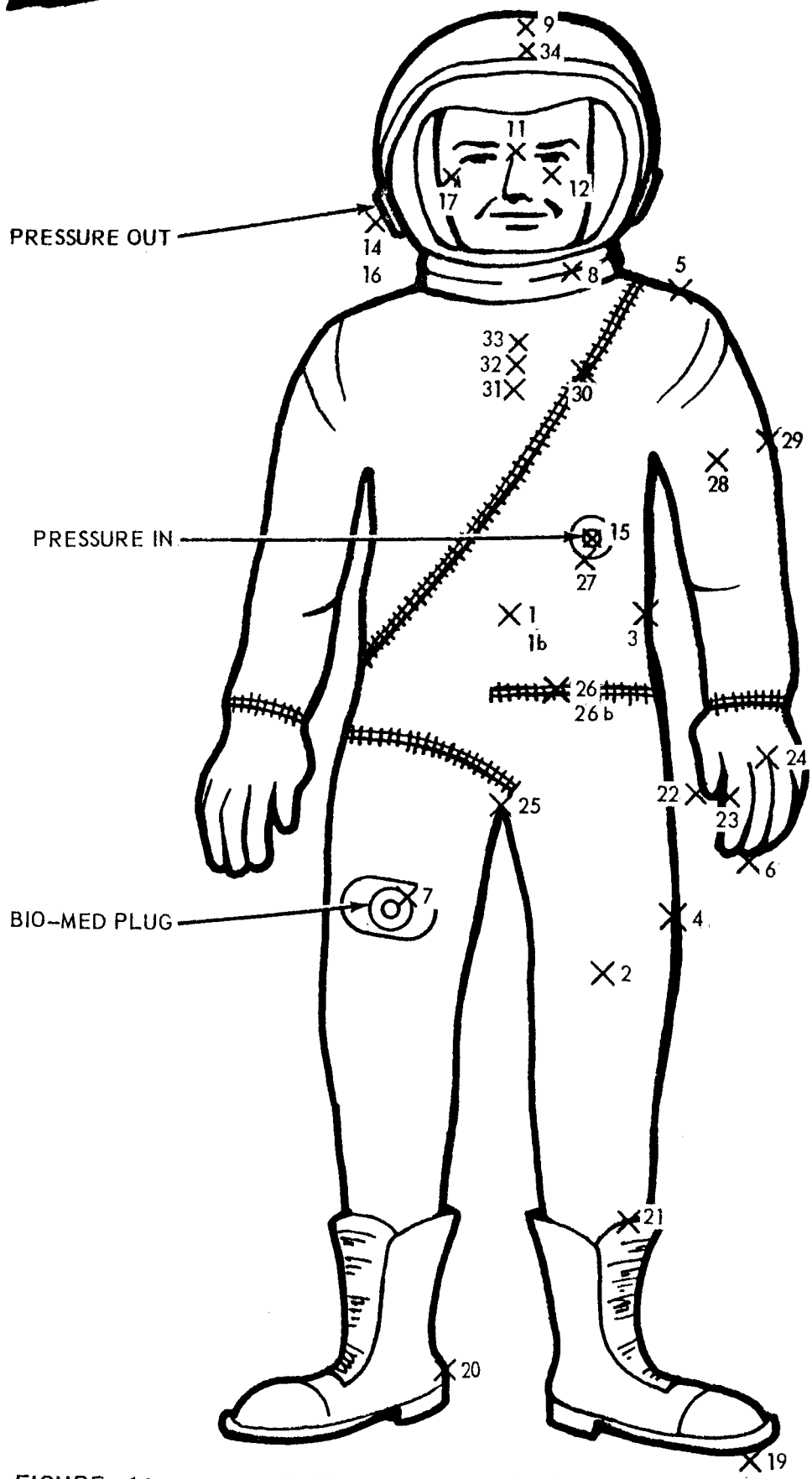

FIGURE 11 INSTRUMENTATION LOCATION , COVERALL OFF

[redacted]

TABLE 2

INSTRUMENTATION LOCATION - COVERALL ON

Depth Position			LOCATION
Outer Surface	Inside Insulation Garment	Inside Pressure Suit	
1-A	1-B 1-C	1-D	Solarplexus, Front
1b-A	1b-B 1b-C	1b-D	Solarplexus, Back
2-A	2-B 2-C	2-D 2-E 2-F	Left Front Thigh
3-A	3-B 3-C	3-D	Left Side 8" Below Arm Pit
4-A	4-B 4-C	4-D	Side of Left Thigh
5-A	5-B 5-C	5-D	Top of Left Shoulder
		6-F	Left Middle Finger Tip
	7-C		Outside of Bio-Medical Plug
	8-C		Helmet Lock Ring, Outside
9-A	9-B 9-C	9-D	Back of Helmet
10-A			Right Upper Arm, Front
10b-A			Right Upper Arm, Back
		11-F	Under Surface of Rubber on Bridge of Nose
		12-D	Inside Clear Visor
	13-C		Inside Colored Visor
		14-E	Outlet Air Temp
		15-E	Inlet Air Temp
		16-A1	Differential Air Pressure

[redacted]

TABLE 2

INSTRUMENTATION LOCATION - COVERALL ON

Depth Position			
Outer Surface	Inside Insulation Garment	Inside Pressure Suit	
		17-A2	Absolute Air Pressure
18-A			Central Upper Chest, Front
18b-A			Central Upper Chest, Back

TABLE 3

INSTRUMENTATION LOCATION - COVERALL OFF

Outer Surface of Pressure Suit	Inside Pressure Suit	Dummy Surface	Location
1-C	1-D		Solarplexus, Front
1b-C	1b-D		Solarplexus, Back
2-C	2-D 2-E	2-F	Left Front Thigh
3-C	3-D		Left Side 8" Below Armpit
4-C	4-D		Side of Left Thigh
5-C	5-D		Top of Left Shoulder
		6-F	Left Middle Finger Tip
7-C			Outside of Bio-Med Plug
8-C			Helmet Lock Ring
9-C	9-D		Back of Helmet
		11-F	Under Surface of Rubber or Bridge of Nose
	12-D		Inside Clear Visor
	14-E		Outlet Air
	15-E		Inlet Air
	16-A1		Differential Air Pressure
	17-A2		Absolute Air Pressure
19-C			Under Tip of Left Toe
20-C			Right Heel
21-C			Top of Left Boot on Zipper
22-C			Left Hand Thumb on Outside
23-C			Left Hand Thumb on Inside
24-C			Left Hand Outside on Buckle
25-C			On Crotch
26-C			Left Waist on Zipper, Front
26b-C			Left Waist on Zipper, Back

TABLE 3
(con't)

Outer Surface of Pressure Suite	Inside Pressure Suit	Dummy Surface	Location
27-C			Inlet Hose Clamp, Outside
28-C			Left Upper Arm Front
29-C			Side of Left, Upper Arm on Buckle
30-C			Upper Central Chest Front, on Zipper
31-C			Upper Central Chest on Harness Metal
32-C			Upper Central Chest, Back
33-C			Upper Central Chest, in Harness Wire
34-C			Front of Helmet, Under Mylar Tape

The temperature indications of 39 thermocouples were recorded continuously on two Brown multipoint recorders. These temperatures were printed out at 0.8 minute intervals throughout the tests. The air inlet and outlet temperatures of the suit were surveyed with a Thwing-Albert manual balance potentiometer. The outlet air temperature was also recorded on one of the Brown recorders. The temperatures of the two remaining thermocouples were recorded on a Consolidated Electrodynamics Corporation recording oscillograph, type 5-114-P3. Figure 12 shows the Brown recorders and the CEC oscillograph.

The absolute pressure of the air at the suit outlet was monitored by a potentiometer type absolute pressure transducer. A strain-gauge type transducer was used to measure the pressure drop between the air inlet and outlet connections. Both pressure indications were recorded on the CEC oscillograph.

3.4.2 Air Flow Equipment

Sufficient instrumentation was provided with the air flow equipment to measure the flow rate and to monitor equipment performance. The air flow rate through the pressure suit was measured by a Fisher-Porter flowmeter. The temperature and pressure pick-up locations are shown in Figure 7.

3.4.3 Space Environment Simulator

The Space Environment Simulator was instrumented for measurement of the chamber pressure, cryogenic wall temperature, orientation of the test article, solar heat flux and spectral distribution. The pressure inside the space chamber was indicated and recorded by a thermal gauge in the high pressure range and by a hot cathode ionization gauge in the lower pressure range. A Consolidated Vacuum Corporation Magnevac was used in the range from atmospheric pressure down to 1 micron and a Consolidated Vacuum Corporation model GIC-110 ionization gauge was used to measure pressures from 10^{-3} mm Hg to ultimate.

Twelve temperatures at selected locations on the cryogenic wall were monitored on a Brown Multipoint recorder. An external switching arrangement was used so that the twelve temperatures could be recorded on eight channels of the recorder.

The orientation of the test article was changed remotely by means of motion gimbal controls on the simulator control panel. A dial position indicator on the panel was used to adjust the orientation. Visual checks through two chamber viewing ports assured the proper orientation after all turns.

Measurements of the solar heat flux and spectral distribution were previously discussed in paragraph 3.3.1.

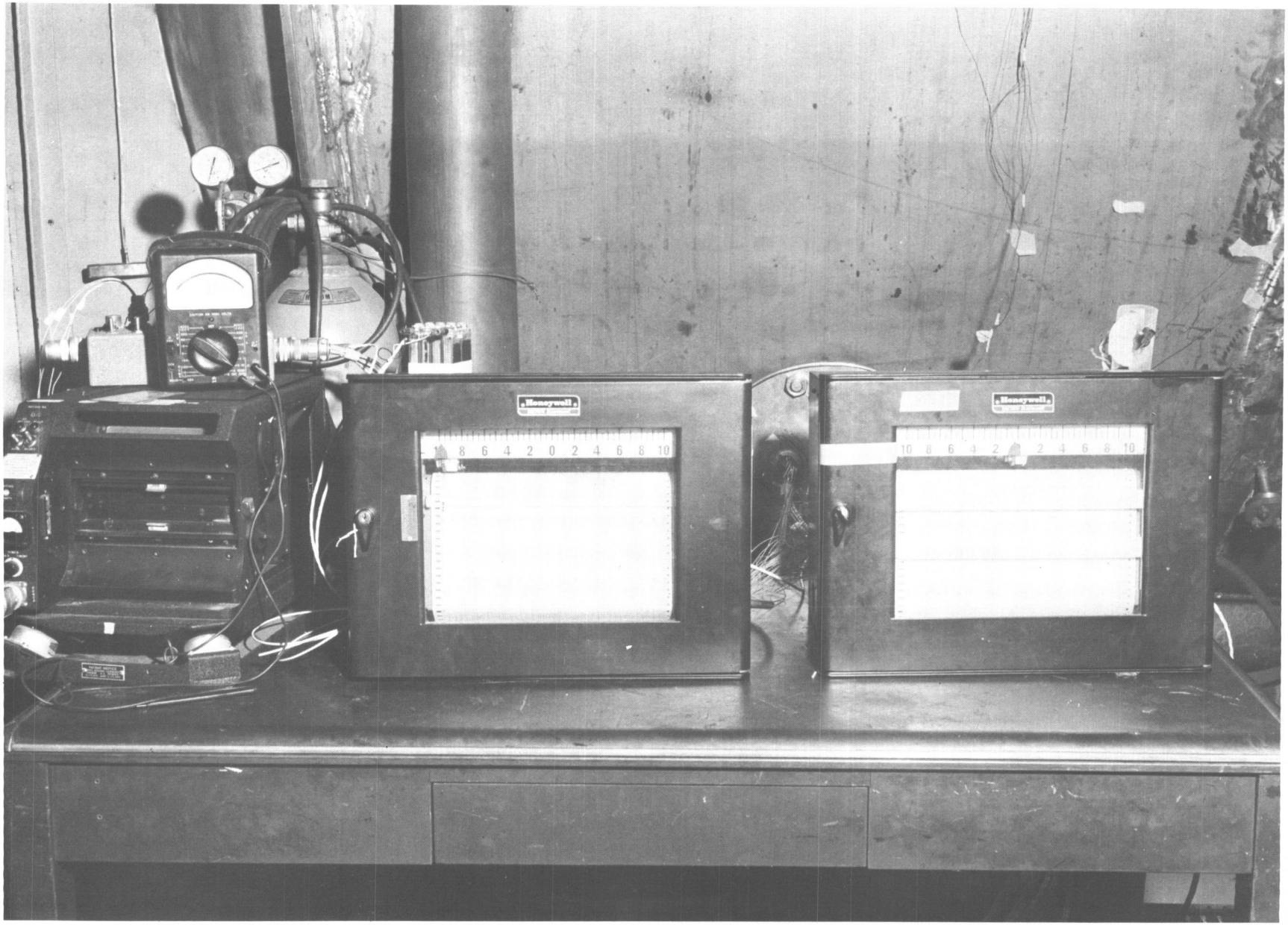

Figure 12 DATA RECORDING EQUIPMENT

[redacted]

3.4.4 Instrumentation Accuracy

The estimated accuracies of the instrumentation used in this test program are as follows:

Temperatures - Brown Multipoint Recorders	±3° F.
Temperatures - CEC Recorder	± 3° F.
Temperatures - Manual Potentiometer	±1° F. (on differential only, not absolute level)
Suit Pressure	±. 1 psi.
Pressure Differential	±. 05 in. Hg
Space Chamber Pressure - at Vacuum Chamber	± 20 %
Solar Flux	± 3 %

3.5 Test Procedure

3.5.1 Preparation of Test Article

One of the major difficulties in preparing the test article was assembling the dummy, pressure suit, and coverall without disrupting the instrumentation. The thermocouples used to measure dummy temperatures were installed prior to the underwear installation. The underwear was then taped in place so that the thermocouples would not be moved during donning of the pressure suit. The instrumentation for the interior of the pressure suit was installed during donning so as to prevent damage to the thermocouples. Instrumentation for the exterior of the suit was installed after donning was completed. A similar procedure was followed for instrumenting the coverall. The junctions of the thermocouples used for measuring the outside surface temperature of the coverall were inserted under the outermost layer of aluminized mylar.

Prior to installation in the Space Environment Simulator, the leakage of the pressure suit assembly was evaluated. The suit outlet was closed and the suit pressurized to approximately 4.0 psig. After the pressure in the suit and suit expansion had been allowed to stabilize, the air make-up required to maintain the suit pressure were measured. The leakage was approximately 900 cc/minute.

Since the measured suit leakage appeared marginal and the exact pumping capacity of the SES was not known, the test article was mounted in the space chamber to determine if sufficient chamber vacuum could be attained. A pressure of approximately 1×10^{-4} mm Hg was obtained. This vacuum was considered sufficient, and final instrumentation checks were then made in preparation for the tests.

3.5.2 Test Conditions

The test program called for data at the seven steady state test points summarized in Table 4 and for the transient responses during several changes from one operating condition to another. Tests involving

[redacted]

[redacted]

TABLE 4

DESIRED TEST POINTS

Run Number	Orientation	Solar Source	Coverall	Tinted Visor Shield
1	Front Facing Solar Wall	Off	On	On
2	Front Facing Sun	On	On	On
3	Left Side Facing Sun	On	On	On
4	Back Facing Sun	On	On	On
5	Front Facing Sun	On	On	Off
6	Front Facing Solar Wall	Off	Off	Off
7	Front Facing Sun	On	Off	Off

Suit Airflow = 15 cfm (inlet condition)

Suit Inlet Temperature = 60^{o} F

Suit Outlet Pressure = 3.5 psia

[redacted]

both the pressure suit and coverall were carried out first. After these tests were completed, the coverall was removed for the remainder of the tests. The thermocouples formerly on the coverall were relocated on the pressure suit.

Steady state was never achieved for test numbers 6 and 7 in Table 4. These tests called for steady state data on pressure suit performance without the coverall.

The tests were terminated prematurely since the safe operating limits were being exceeded and there was a possibility of destroying the pressure suit. The safe operating limits were considered to be 32° F and 160° F. for the inner surface of the pressure suit.

The test conditions for each of the steady state test points for which data were taken are summarized in Table 5. The air flow conditions were held as constant as possible throughout the test program and changed negligibly during the transient temperature surveys. The data were taken over a period of four days of testing. A log of the test program events for all four days of testing is presented in Table 6. The points at which the steady state data surveys were taken are also indicated.

TABLE 5

STEADY STATE CONDITIONS

Orientation	Solar Source	Coverall	Tinted Visor Shield	Chamber Pressure mm Hg	Chamber wall Temperature ^{o}F	Suit Pressure PSIA	Suit Airflow CFM
Front Facing Sun	Off	On	On	7×10^{-5}	-310	2.95	17.9
Front Facing Sun	Off	On	Off	9×10^{-5}	-310	3.47	15.2
Front Facing Sun	On	On	On	9×10^{-5}	-310	3.45	16.0
Front Facing Sun	On	On	Off	9×10^{-5}	-310	3.48	15.5
Left Side Facing Sun	On	On	On	8×10^{-5}	-310	3.45	16.0
Back Facing Sun	On	On	On	8×10^{-5}	-310	3.42	15.7
Back Facing Sun	On	Off	Off	8×10^{-5}	-310	3.47	15.6

TABLE 6

TEST LOG

1st Day	
5:05 a. m.	Mechanical pump on
5:58	Ejector pump on
6:47	Oil diffusion pumps on
7:00	Started suit airflow
10:43	Started cooldown
11:28	Wall cooled to -310°F
2:55 p. m.	Data reduced for steady state, no sun, coveralls on, tinted visor on (Figure 17)
3:42	Lamps turned on, model facing sun
4:25	All lamps up to full power
4:40	Turned model 180°to back facing sun
4:55	Lamps off, liquid nitrogen pumps off
5:00	Oil diffusion pumps off
5:15	Ejector pump off
6:40	Mechanical pump off
2nd Day	
7:05 a. m.	Mechanical pump on
8:02	Ejector pump on
8:17	Oil diffusion pumps on
8:40	Started suit airflow
9:12	Started cooldown
9:58	Wall cooled to -310° F
10:15	Lamps on, back to sun
11:05	All lamps up to full power

2nd Day (Cont'd)

12:02 p. m.	Data reduced for steady state, back to sun, coveralls on, tinted visor on (Figure 22)
12:06	Turned model 90° to left side facing sun
1:16	Data reduced for steady state, left side to sun, coveralls on, tinted visor on (Figure 21)
1:20	Turned model 90° to front facing sun
2:48	Data reduced for steady state, front to sun, coveralls on, tinted visor on (Figure 19)
2:50	Turned model 180° to back facing sun
3:07	Liquid nitrogen pump off, diffusion pumps off
3:30	Ejector pump off
4:22	Lamps off
4:50	Mechanical pump off

3rd Day

9:57 a. m.	Mechanical pump on
10:42	Ejector pump on
11:05	Pil diffusion pumps on
12:05 p. m.	Started suit airflow
12:10	Started cooldown
1:24	Wall cooled to -310° F
2:22	Data reduced for steady state, no sun, coveralls on, tinted visor off (Figure 18)
2:23	Lamps on, front facing sun
2:42	Lost power
2:50	Vented suit to chamber
2:52	Power on, all pumps on
3:20	Lamps on
3:55	All lamps up to full power

[redacted]

3rd Day (Cont'd)

4:58	Data reduced for steady state, front to sun, coveralls on, tinted visor off (Figure 20)
5:00	Oil diffusion pumps off
5:22	Suit airflow off
6:19	Lamps off
6:40	Mechanical pump off

4th Day

11:23 a. m.	Mechanical pump on
12:12 p. m.	Ejector pump on
12:25	Oil diffusion pumps on
1:07	Started suit airflow
2:05	Started cooldown
2:38	Wall cooled to -310^{o} F
2:38	Lamps on, front facing sun
3:00	Turned model 180^{o} to back facing sun
3:05	Lamps up to power
3:43	Data reduced for steady state, back to sun, coveralls off, tinted visor off (Figure 23)
3:45	Turned model 180^{o} to front facing sun
4:00	Reduced lamp power to 1300 watts
4:01	Turned model 180^{o} to back facing sun
4:03	Liquid nitrogen pumps off
4:06	Oil diffusion pumps off
4:22	Ejector pump off
5:25	Lamps off
5:40	Mechanical pump off

[redacted]

4.0 DISCUSSION OF RESULTS

4.1 Coverall Effectiveness

4.1.1 Temperature Distributions

The effectiveness of the insulated coverall garment can be shown qualitatively by the temperature distributions over the surface of the coverall and by temperature profiles through the coverall and pressure suit materials. These temperatures were recorded continuously during the tests.

Typical outside surface temperatures of the coverall are shown in Figure 13 for the 2nd day of testing. A log of events for the day is included on the figure to explain the behavior of the temperatures. The times at which steady state data surveys were made are also shown in this figure. When the simulated solar heating was turned on, very large temperature differences developed between the illuminated and shaded sides of the coverall garment. The outside surface temperatures approached steady state values about one hour after a change in environmental conditions or orientation of the model was made.

The transient temperatures on the front solarplexus area of the coverall and the pressure suit are shown in Figure 14. This figure shows that the variations in temperature on the inside of the coverall and pressure suit are much smaller than on the outside of the coverall. The times required for these transients to die out are also much longer. As an example, one hour after the turn to orient the front of the test article toward the sun, (228 minutes in Figure 14) the outside coverall surface temperatures had very nearly approached steady state values. The coverall inside temperature, however, had not quite reached steady state after 1-1/2 hours. The response of the pressure suit was even slower. In actual space maneuvers the slowness of these internal responses could be very advantageous.

Further evidence of the effectiveness of the coverall may be shown by studying the temperatures on the unprotected pressure suit. The pressure suit outside surface temperatures are shown in Figure 15 during tests without the coverall. Steady state was not reached with the suit facing the sun because internal suit temperatures exceeded the permissible maximum of 160°F. When the temperatures on the front of the suit exceeded the pre-determined maximum, the suit was turned so the back faced the sun (42 minutes, Figure 15). Temperatures with the back of the suit illuminated did not get as high as when the front of the suit was illuminated. This may be attributed to uneven air flow distribution in the pressure suit or local differences in radiation properties of the suit.

The transient response of the unprotected pressure suit temperatures was much more rapid than the response of the temperatures with the coverall on. Temperatures on the outside of the pressure suit approached steady state values in about 1/2 hour. The more rapid

FIGURE 13

COVERALL OUTER SURFACE THERMAL BEHAVIOR DURING 2ND DAY OF TESTING

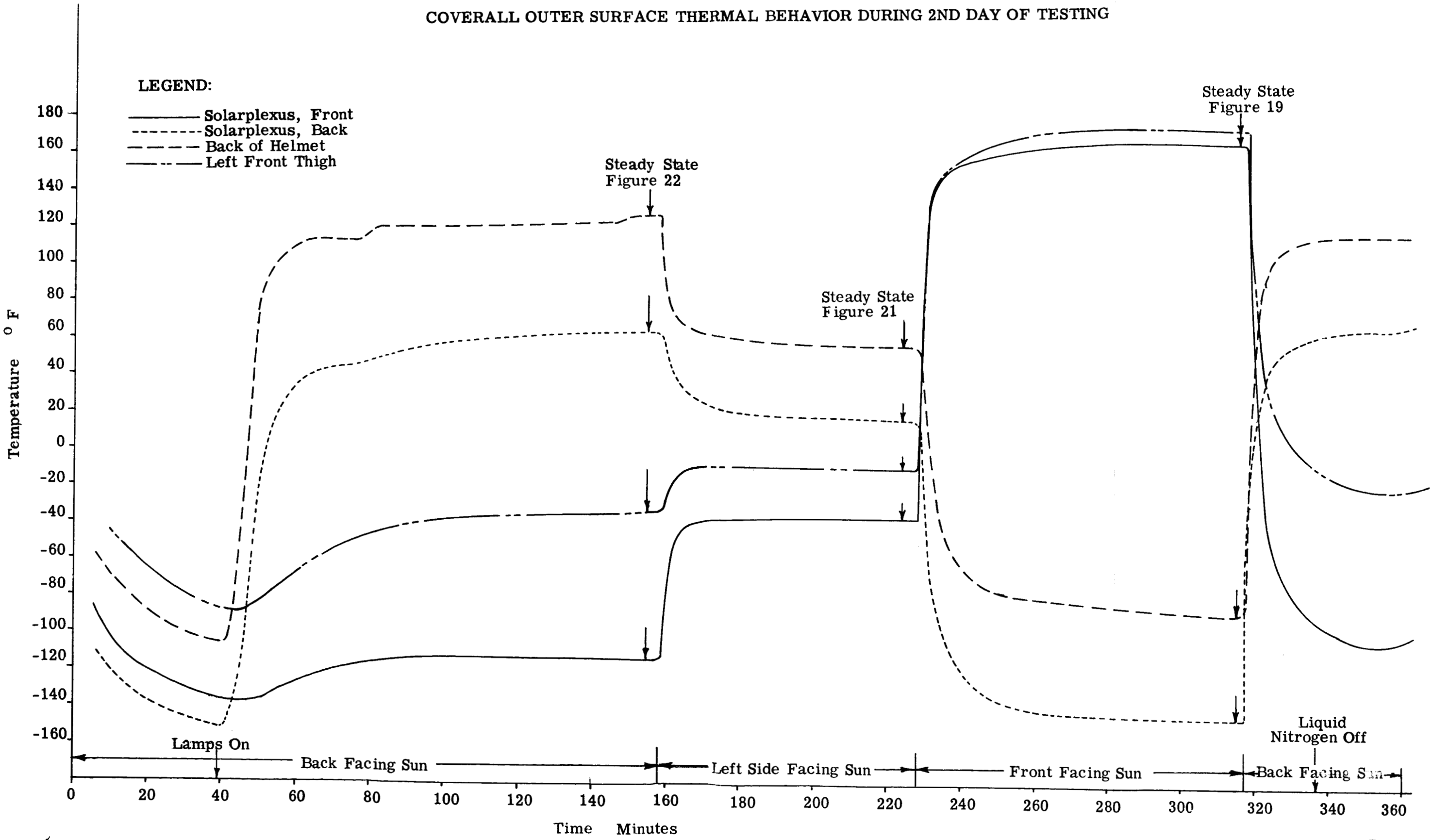

FIGURE 14

TEMPERATURE PROFILE AT SOLARPLEXUS FRONT DURING 2ND DAY OF TESTING

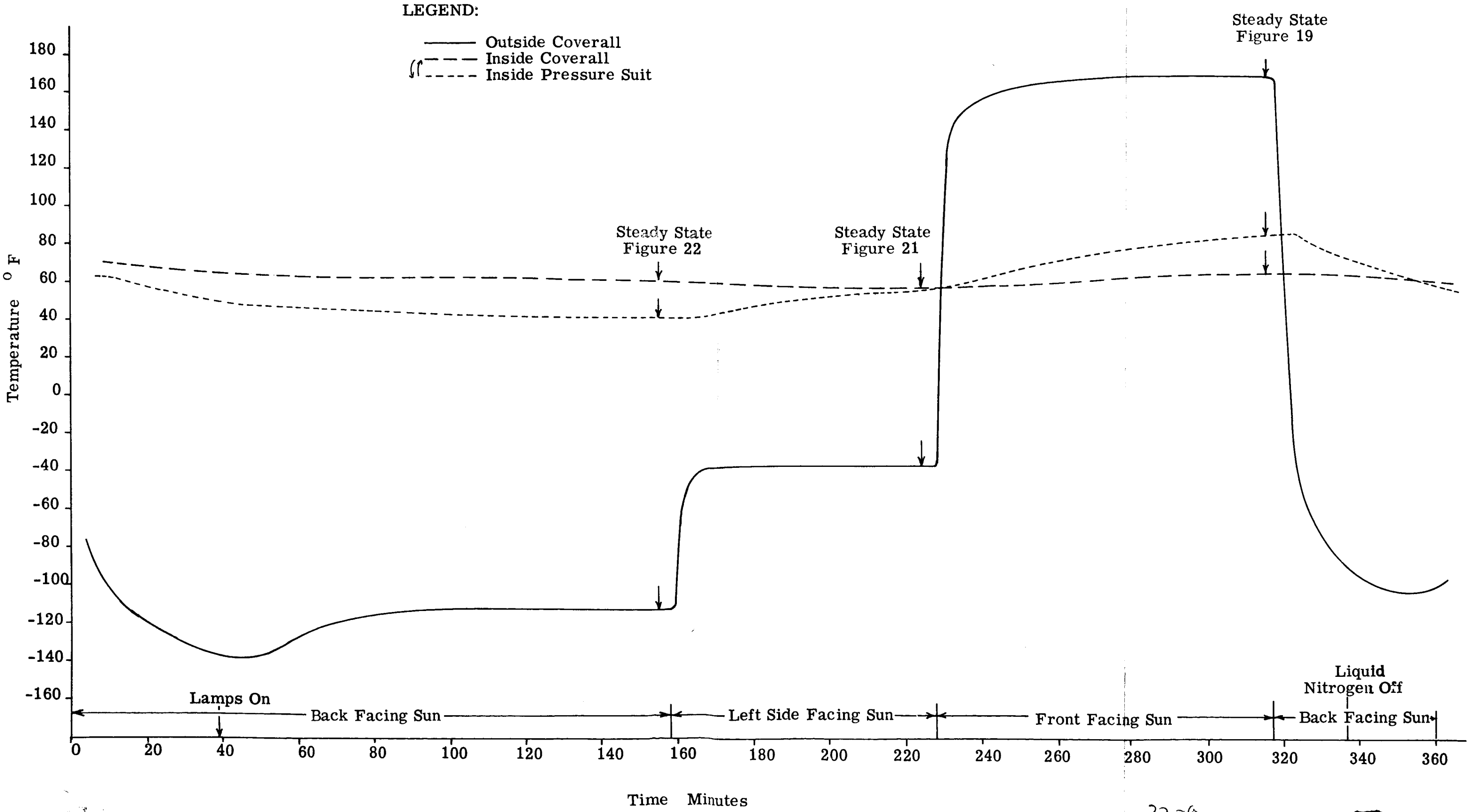

FIGURE 15

PRESSURE SUIT OUTER SURFACE THERMAL BEHAVIOR WITHOUT COVERALL

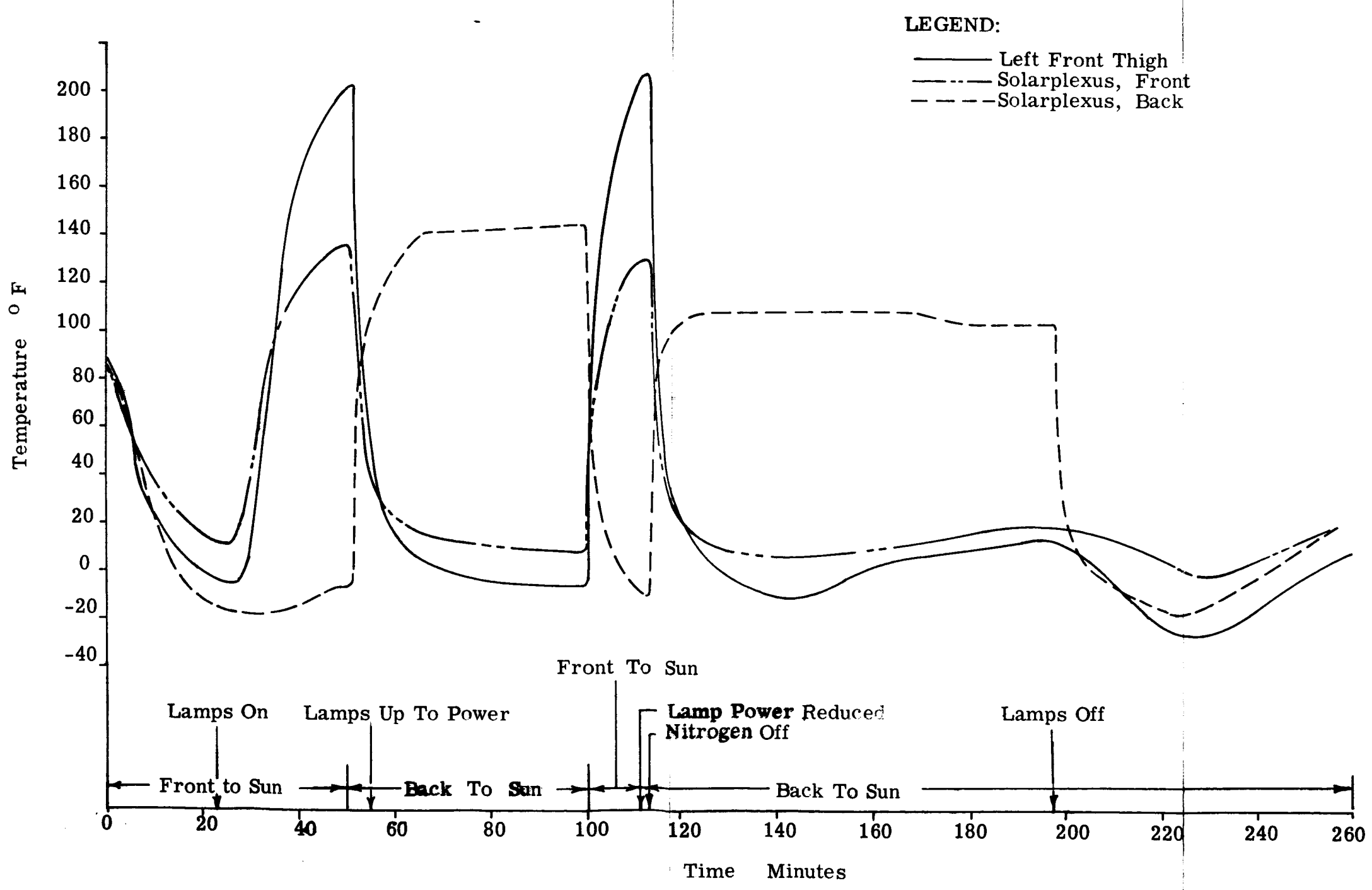

response of the suit inner surface temperature and the dummy temperature is shown by Figure 16. The temperatures of the pressure suit inside surface approached steady state in about 30 - 45 minutes. The dummy surface temperature did not reach steady state conditions during the test.

4.1.2 Temperature Profiles

The resistance to heat transfer of the coverall garment may be compared to the resistance of the pressure suit by examining temperature profiles through the coverall and pressure suit materials. These temperature profiles have been obtained for the seven steady state test points and are presented in Figures 17 through 23. The results are also tabulated in Tables 7 and 8.

Two tests were conducted in a cold environment (no solar heating) with the coverall on. The results are shown in Figures 17 and 18. The tests differed in that a gold tinted visor shield used for the first test (Figure 17) was removed for the latter test (Figure 18). The repeatability of the coverall and pressure suit test data is very good even though the tests were run on different days.

The temperature change through the coverall was approximately 200°F compared to 2 to 5°F temperature change across the pressure suit. This indicates the coverall is very effective, having a thermal resistance 40 to 100 times the resistance of the pressure suit.

There appears to be considerable scatter in the insulated coverall outside temperatures even though there was no solar heating. Some scatter was expected in the cold environment because the surface temperature is sensitive to the heat transferred through the coverall, the coverall surface radiative properties, and the geometry of the surface. Additional data scatter was expected because of the non-homogeneity of the coverall and because of the irregularity of the coverall surface.

Another sizeable difference in temperature may occur where the aluminized surface of the mylar outer layer is exposed to the cold environment rather than the mylar side. Except for a narrow strip on the back of the helmet cover and one hand mitten, all of the instrumented coverall had the mylar side exposed.

The dummy left finger temperature, point number 6, Figure 17-23, varied considerably more from test to test than other parts of the dummy surface as indicated by the other temperature profiles. This variation probably occurred due to the low heat capacity of the finger and poor air circulation in the left glove. Upon disassembly of the pressure suit, (after tests had been completed), it was observed that the air duct supplying air to the left glove was folded. Therefore, very little air was circulated through the glove and the temperature was not controlled as closely as other parts of the dummy.

FIGURE 16

TEMPERATURE PROFILE AT LEFT FRONT THIGH, COVERALL OFF

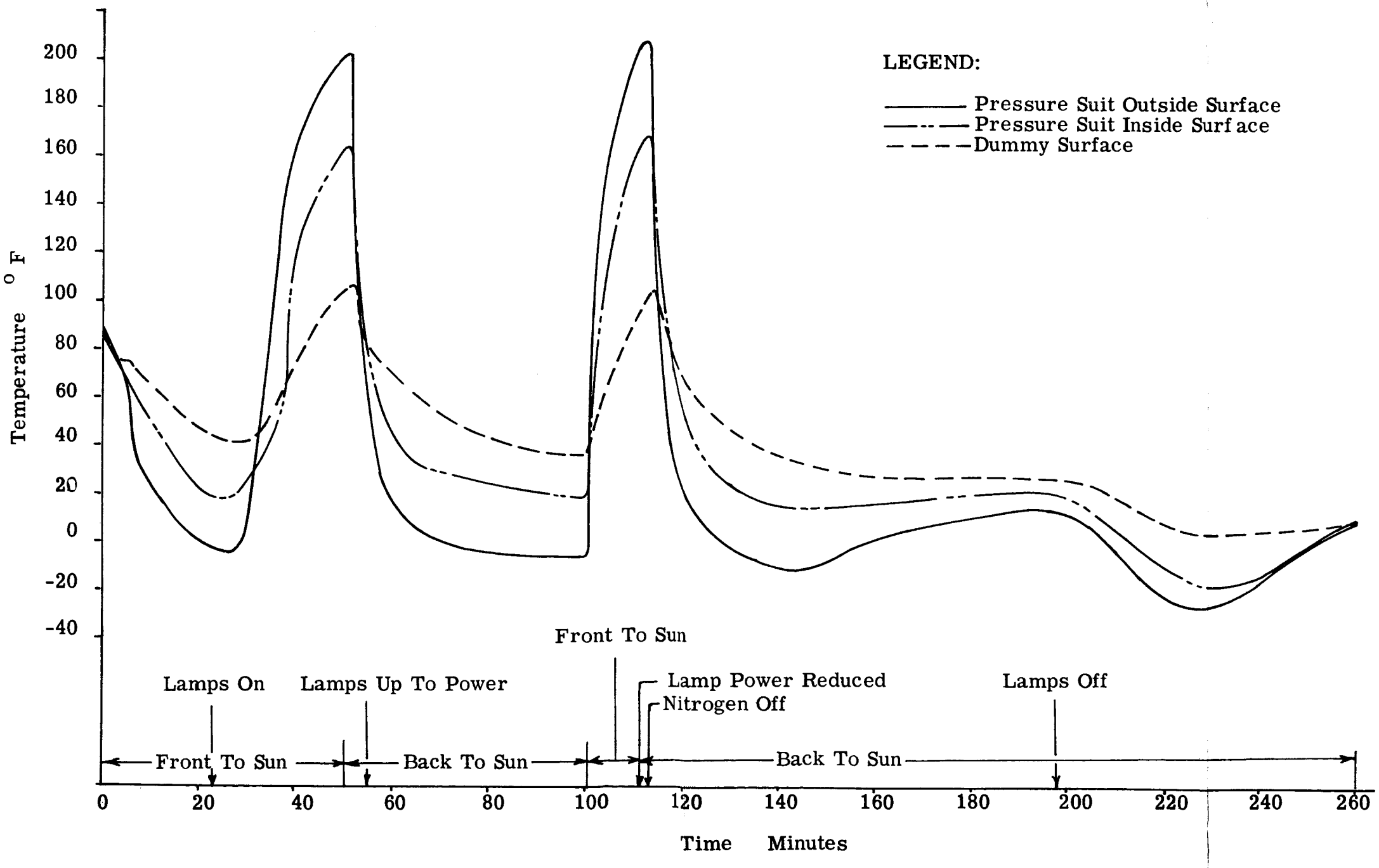

FIGURE 17

SUIT TEMPERATURE SURVEY AT STEADY STATE

NO SUN
COVERALLS ON - COLORED VISOR ON

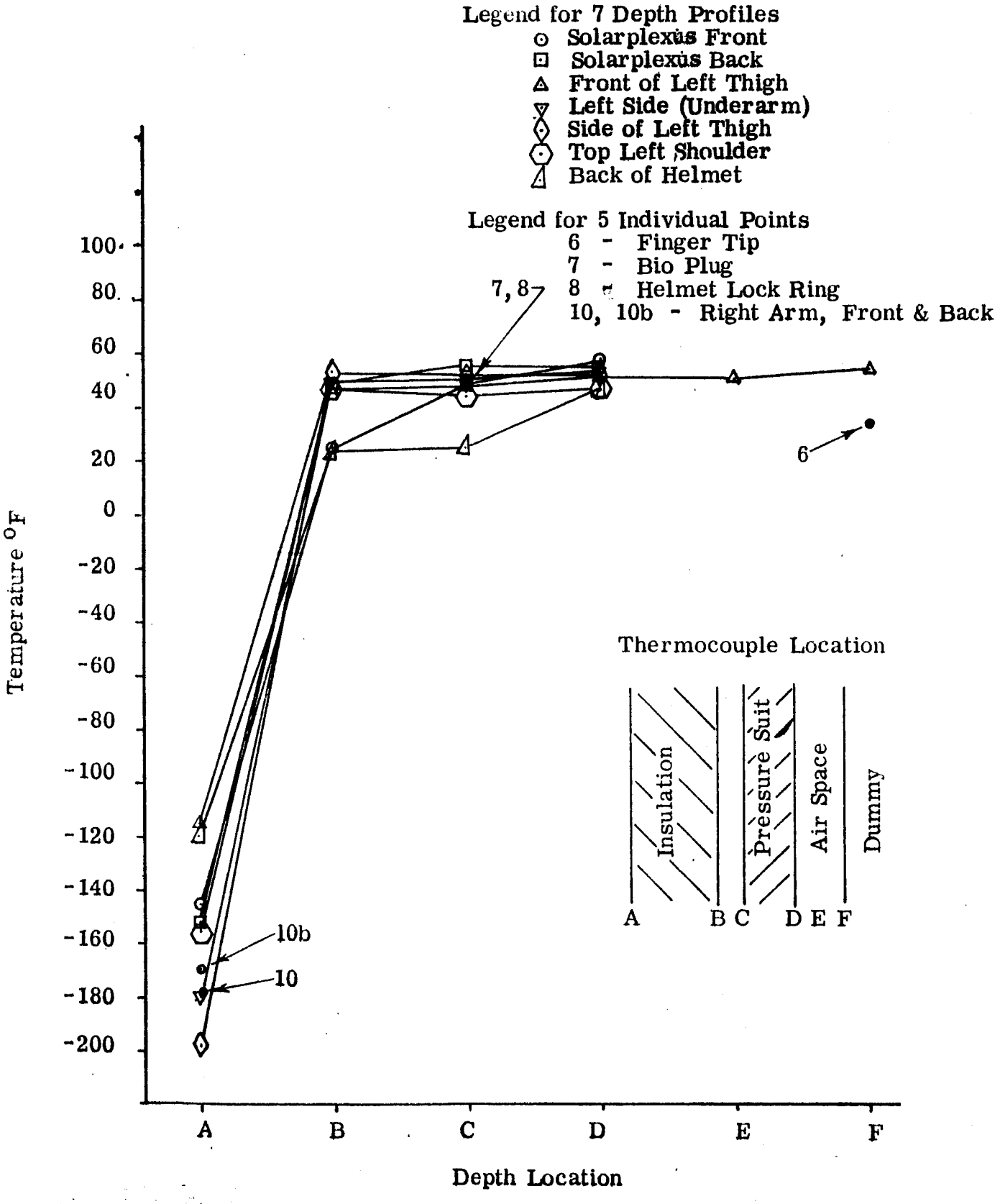

[redacted]

FIGURE 18

SUIT TEMPERATURE SURVEY AT STEADY STATE

NO SUN
COVERALLS ON - COLORED VISOR OFF

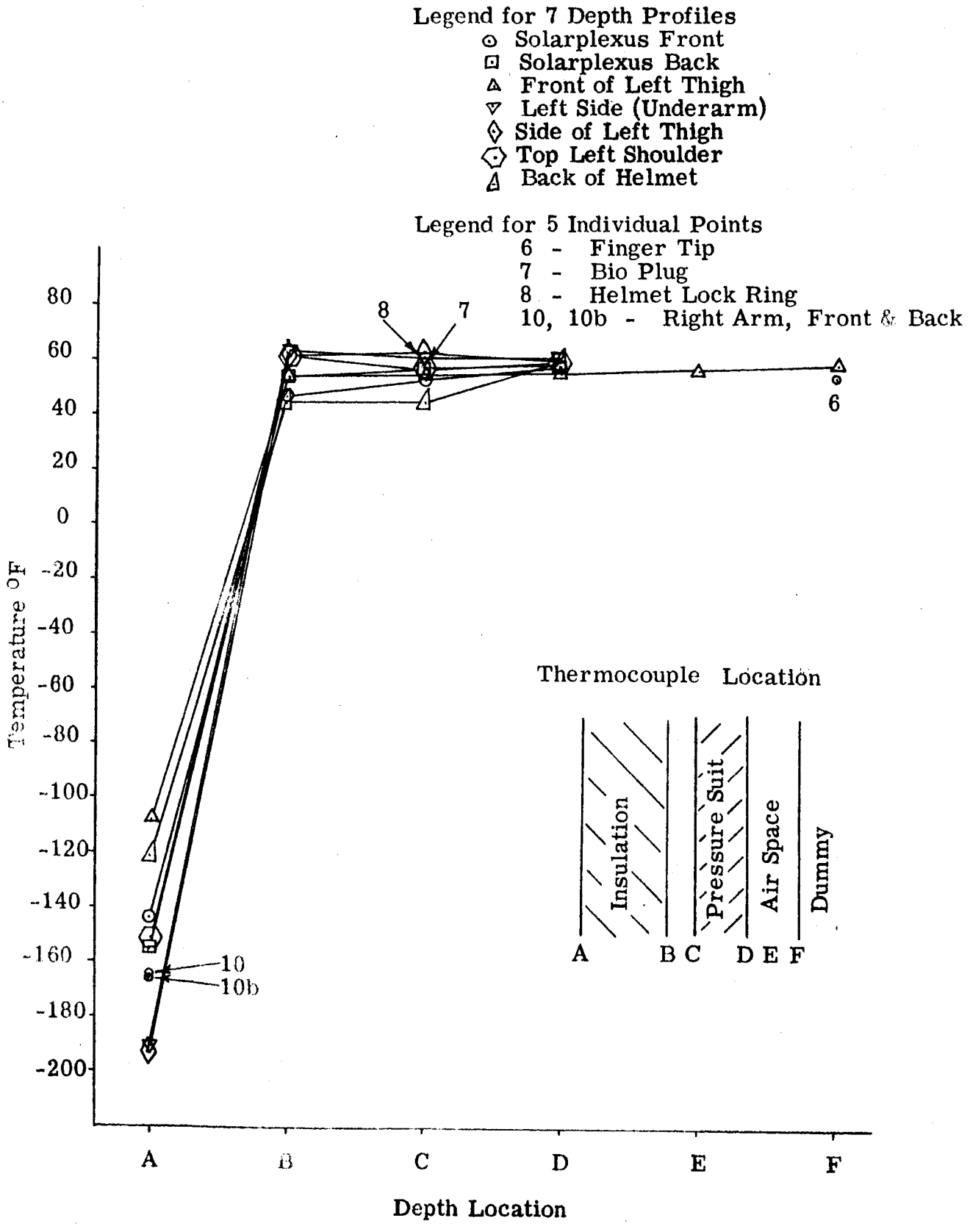

[redacted]

FIGURE 19

SUIT TEMPERATURE SURVEY AT STEADY STATE

SUN ON FRONT OF MODEL
COVERALLS ON - COLORED VISOR ON

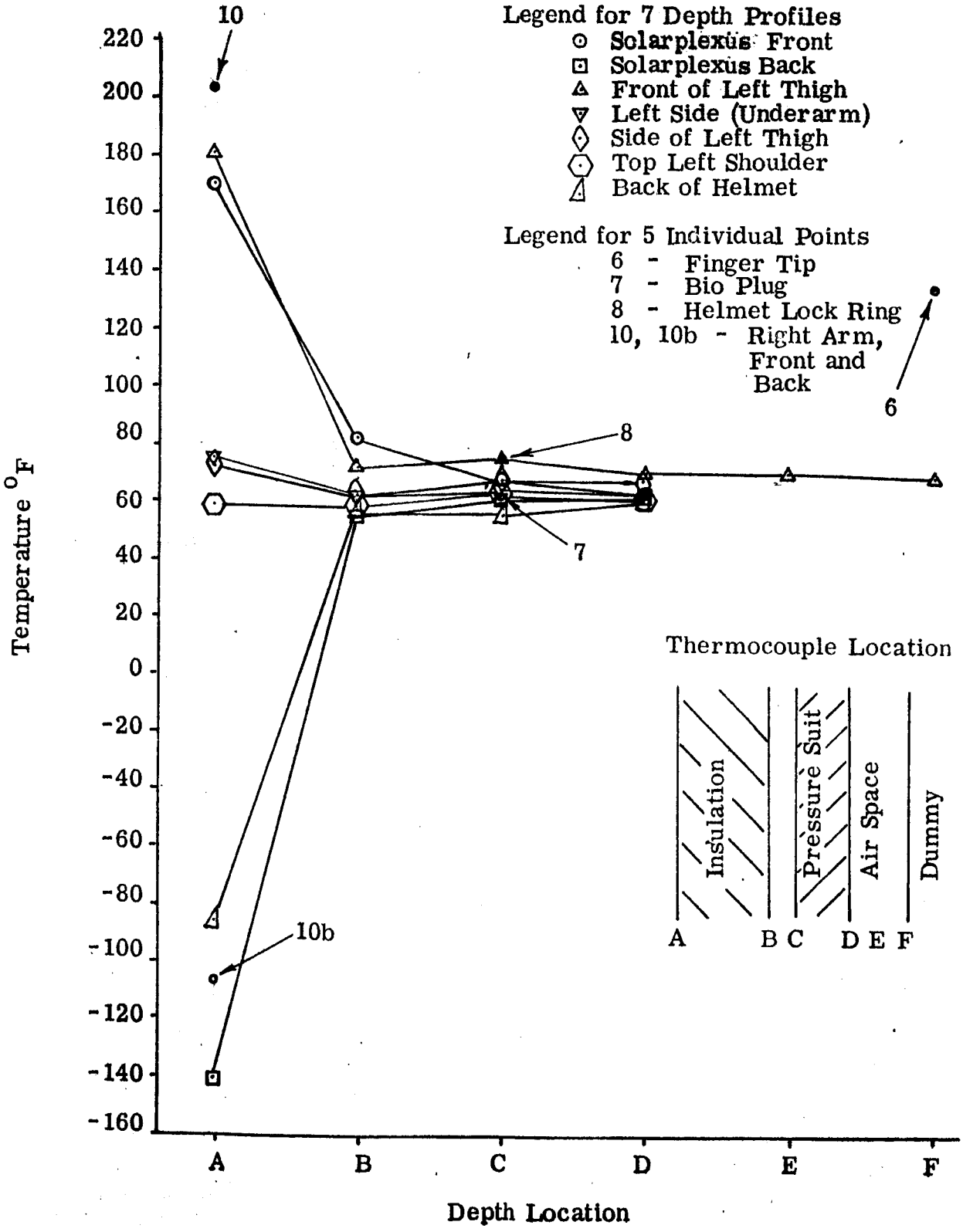

[redacted]

[redacted]

FIGURE 20

SUIT TEMPERATURE SURVEY AT STEADY STATE

SUN ON FRONT OF MODEL
COVERALLS ON - COLORED VISOR OFF

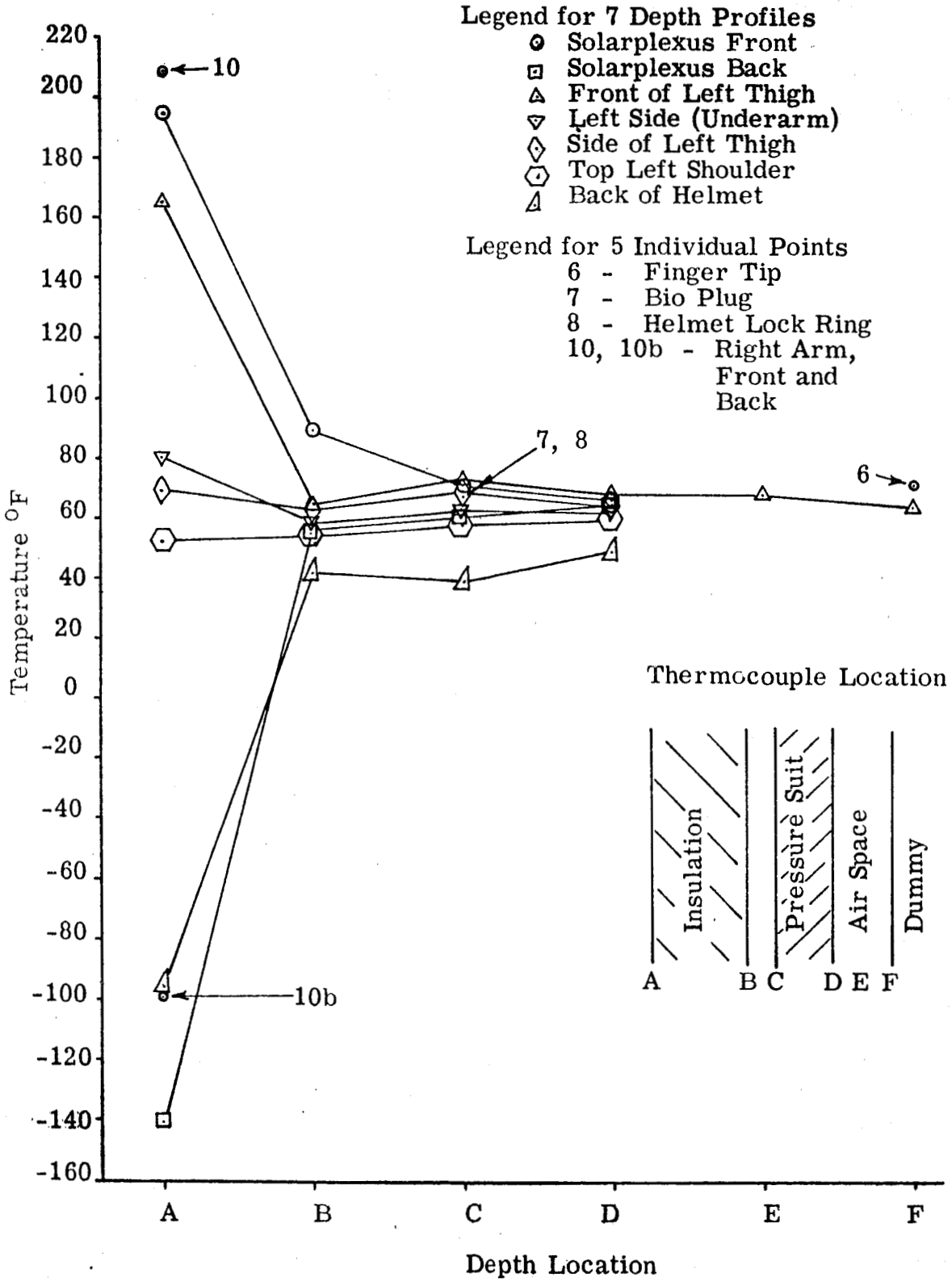

[redacted]

FIGURE 21

SUIT TEMPERATURE SURVEY AT STEADY STATE

SUN ON LEFT SIDE OF MODEL
COVERALLS ON - COLORED VISOR ON

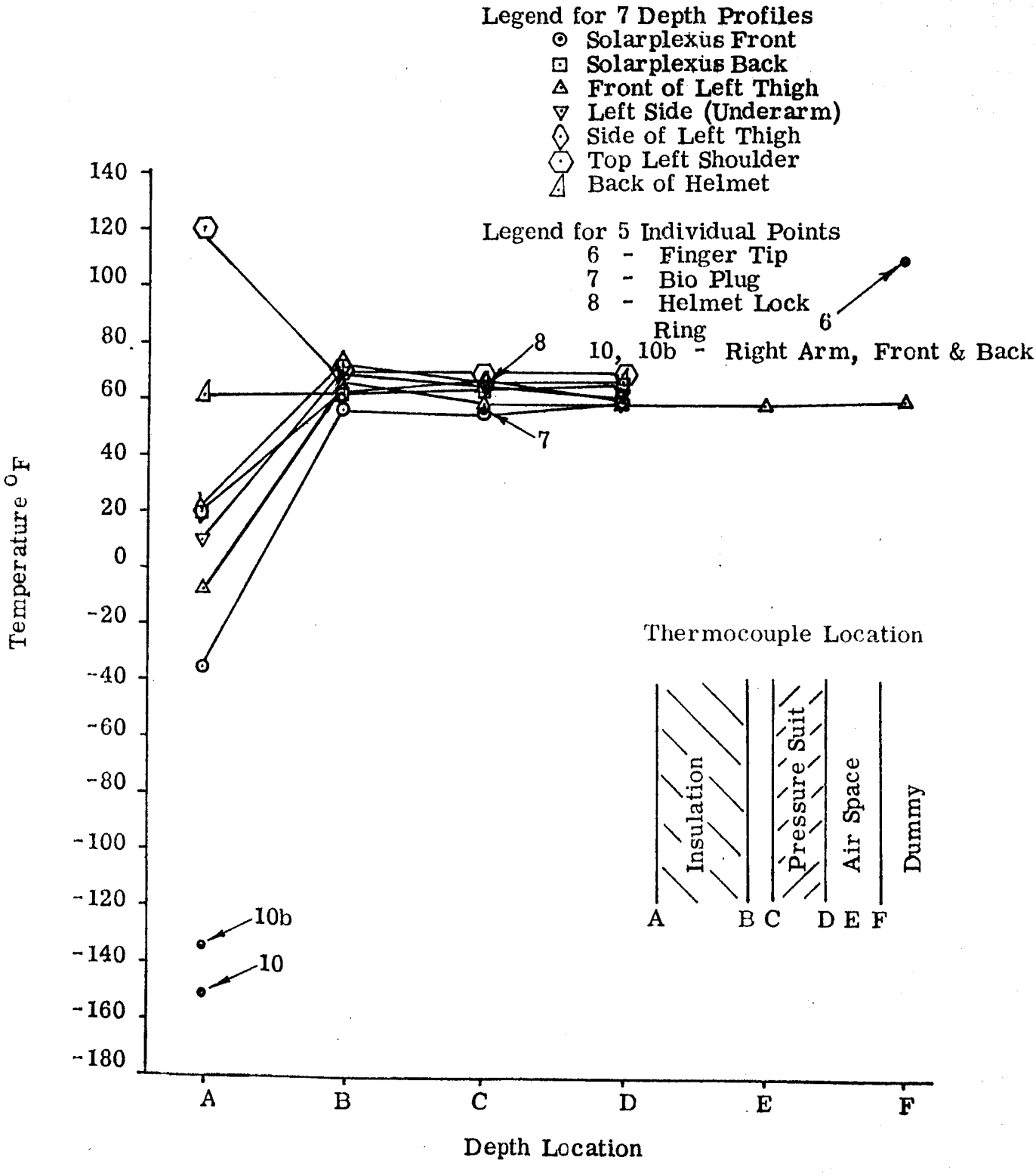

FIGURE 22

SUIT TEMPERATURE SURVEY AT STEADY STATE

SUN ON BACK OF MODEL
COVERALLS ON - COLORED VISOR ON

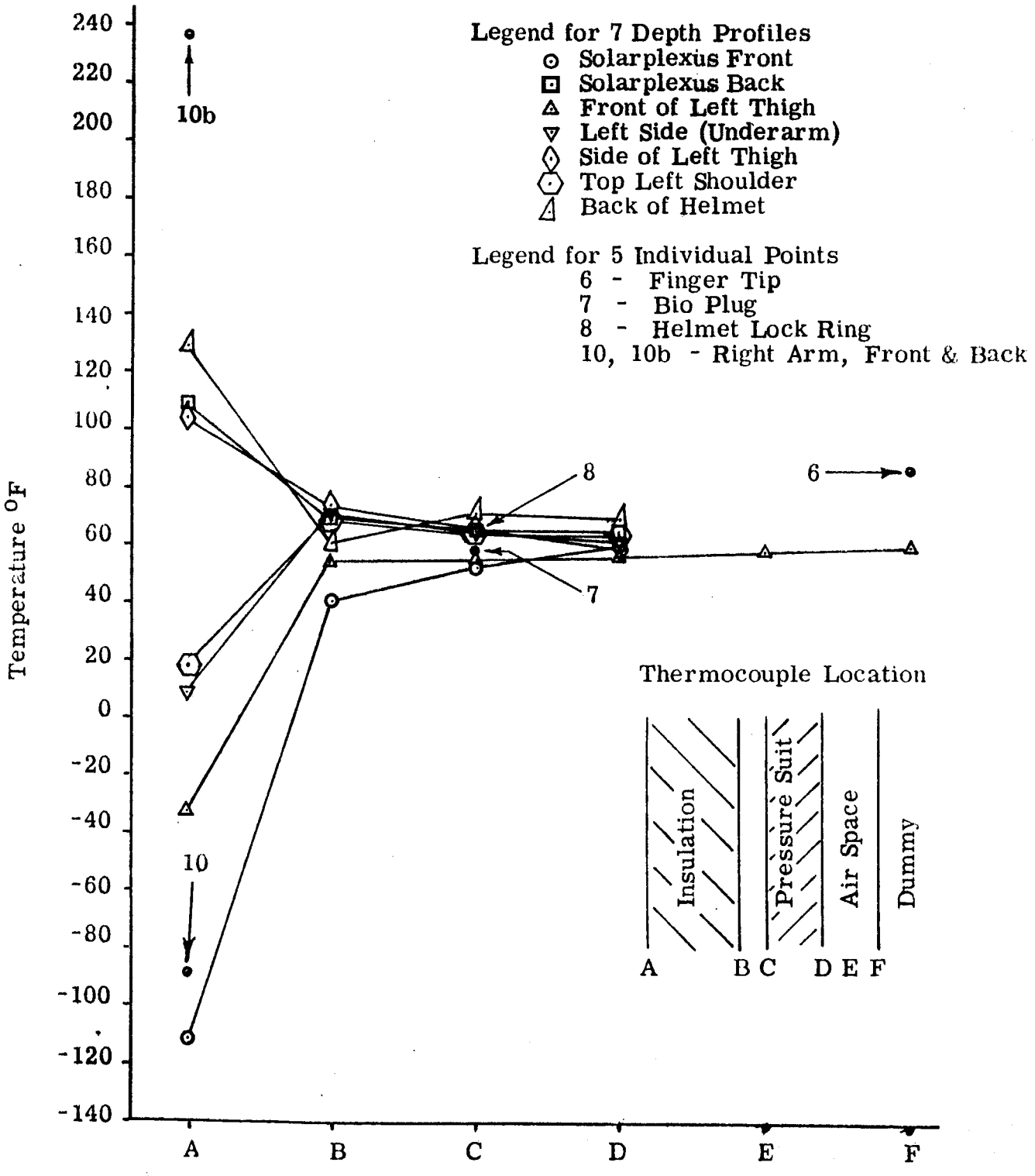

FIGURE 23

SUIT TEMPERATURE SURVEY AT STEADY STATE

SUN ON BACK OF MODEL
COVERALLS OFF - COLORED VISOR OFF

Legend for 7 Depth Profiles

- ⊙ Solarplexus, Front
- ⊡ Solarplexus, Back
- △ Thigh, Left Front
- ▽ Left Side, 8" Below Armpit
- ◇ Side of Left Thigh
- ⬡ Top of Left Shoulder
- ⧋ Back of Helmet

Legend for 17 Individual Points

- 6 - Left Middle Finger Tip
- 7 - Outside of Bio-Medical Plug
- 8 - Helmet Lock Ring, Outside
- 19 - Under Tip of Left Toe
- 20 - Heel of Right Foot
- 21 - Top of Left Boot on Zipper
- 22 - Left Hand Thumb, on Outside
- 23 - Left Hand Thumb, on Inside
- 24 - Left Hand Outside on Buckle
- 25 - On Crotch
- 26 - Left Waist on Zipper, Front
- 26b - Left Waist on Zipper, Back
- 28 - Left Upper Arm, Front
- 29 - Side of Left Upper Arm on Buckle
- 31 - Central Upper Chest on Harness Metal
- 32 - Upper Central Chest, Back
- 33 - Upper Central Chest, In Harness Wire

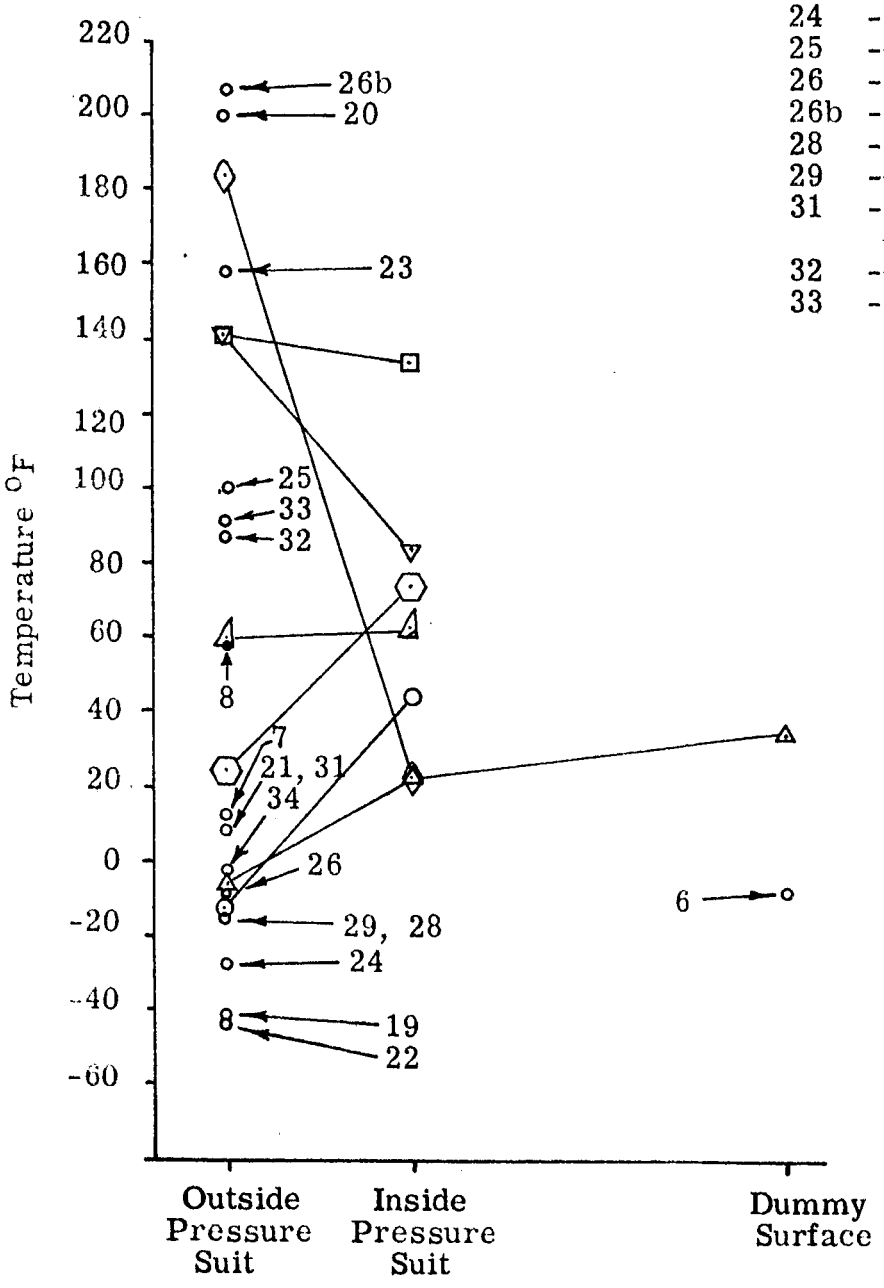

[redacted]

[redacted]

TABLE 7

STEADY STATE TEMPERATURE SURVEY - COVERALL ON

Location	Thermocouple Number	Temperature °F					
		Fig. 17	Fig. 18	Fig. 19	Fig. 20	Fig. 21	Fig. 22
Solarplexus, Front	1-A	-145	-144	170	194	- 36	-112
	1-B	27	47	82	89	56	40
	1-C	49	53	67	71	55	52
	1-D	58	59	63	66	59	59
Solarplexus, Back	1b-A	-152	-154	-141	-141	19	109
	1b-B	49	54	55	51	61	69
	1b-C	55	57	60	58	63	65
	1b-D	55	58	62	56	65	65
Left Front Thigh	2-A	-180	-191	75	81	9	9
	2-B	48	55	72	64	65	55
	2-C	48	55	75	73	58	55
	2-D	51	56	70	68	58	56
	2-E	51	58	70	68	58	58
	2-F	55	60	69	64	60	60
Left Side 8" Below Arm Pit	3-A	-115	-109	180	165	- 8	- 33
	3-B	50	61	62	58	69	71
	3-C	52	61	64	63	65	65
	3-D	54	62	64	62	62	62
Side of Left Thigh	4-A	-198	-192	72	70	19	103
	4-B	53	64.5	63	63	72	73
	4-C	52	64	67	69	67	66
	4-D	52	63	67	65	60	60
Top of Left Shoulder	5-A	-156	-151	59	53	118	18
	5-B	47	60	58	54	69	68
	5-C	44	57	62	58	69	64
	5-D	48	61	61	59	69	64
Left Middle Finger Tip	6-F	35	55	134	71	109	86
Outside of Bio-Medical Plug	7-C	50	58	65	68	55	58
Helmet Lock Ring, Outside	8-C	50	60	73	67	65	66
Back of Helmet	9-A	-120	-121	- 86	- 96	60	128
	9-B	24	44	56	42	62	60
	9-C	25	45	55	39	66	71
	9-D	47	60	60	49	67	69
Right Upper Arm, Front	10-A	-179	-166	202	208	-152	- 90
Right Upper Arm, Back	10b-A	-169	-165	-107	- 99	-135	235

[redacted]

TABLE 8

STEADY STATE TEMPERATURE SURVEY - COVERALL OFF

Location	Thermocouple Number	Temperature °F
Solarplexus, Front	1-C	- 13
	1-D	43
Solarplexus, Back	1b-C	142
	1b-D	134
Left Front Thigh	2-C	- 6
	2-D	20
	2-E	24
	2-F	34
Left Side Below Armpit	3-C	142
	3-D	83
Side of Left Thigh	4-C	183
	4-D	22
Top of Left Shoulder	5-C	24
	5-D	73
Left Middle Finger Tip	6-F	- 8
Outside of Bio-Medical Plug	7-C	12
Helmet Lock Ring	8-C	59
Back of Helmet	9-C	60
	9-D	62
Under Tip of Left Toe	19-C	- 42
Right Heel	20-C	199
Top of Left Boot on Zipper	21-C	8
Left Hand Thumb on Outside	22-C	- 44
Left Hand Thumb on Inside	23-C	158
Left Hand Outside on Buckle	24-C	- 28
On Crotch	25-C	100
Left Waist on Zipper, Front	26-C	- 10
Left Upper Arm, Front	28-C	- 16
Side of Left Upper Arm on Buckle	29-C	- 16
Central Upper Chest on Harness Metal	31- C	8
Upper Central Chest, Back	32-C	86
Upper Central Chest in Harness Wire	33-C	91

Two tests were also made for the front of the test article facing the sun with the coverall on. The tinted visor shield was removed during the latter test. The results for both tests are shown in Figures 19 and 20. Exposure of one side of the coverall to solar heating and the other to the cold of space resulted in very large temperature differences on the outside surface of the coverall. The temperatures varied from -140°F to +210°F. The high reproducibility of the coverall and pressure suit thermal data during tests on separate days is shown in these two figures.

All of the outside coverall surface temperatures in Figures 19 and 20 are higher than the temperatures during the tests in the cold environment, Figures 17 and 18. The higher surface temperatures on the back side of the coverall was probably due to reflected solar energy in the simulator. There was not sufficient difference in pressure suit air temperature to account for such changes in surface temperature.

Although the outside of the coverall experienced a wide variation in temperature, the inside surface of the pressure suit did not show variations over approximately 10° F from one location to another. The small temperature variation on the inside of the pressure suit is desirable for the comfort of the crewman. The small variation also indicates the thermal effectiveness of the coverall garment.

Figure 21 shows the temperature profiles obtained for a test with the left side of the coverall exposed to solar heating. Except for two temperature locations, front and back of the right arm, the temperature variation of the coverall surface was much less than during the previous tests. The apparent decrease in outside surface temperature variation occurred because most of the thermocouples were located on the front and back of the test article and received similar environmental heating. The thermocouples on the right arm indicated low temperatures because they were shaded from the sun.

Two temperature profiles were obtained with the back of the test article toward the sun, coverall on and coverall off. The temperature profile with the coverall on is shown in Figure 22. This profile is similar to figures 19 and 20, except that the hot and cold temperatures are on the opposite sides of the coverall. The temperatures in Figure 22 for the left side of the coverall are slightly lower than in Figures 19 and 20. This is probably due to the irregularity in the coverall surface and the shadow effects of the arm.

The temperature profile for the unprotected pressure suit with back toward the sun is shown in Figure 23. The maximum outside surface temperature of the pressure suit is approximately the same as the maximum coverall temperature in Figure 22. The cold side temperatures in Figure 23 are much higher however, indicating a higher rate of heat loss. The maximum temperature variation of the pressure suit outer surface in Figure 23 is about 250°F as compared to about 350°F in Figure 22. An even wider difference exists in the

pressure suit inside temperature, which directly influences the comfort of the worker. For the test without the coverall, the inside temperature variation was about 115°F. This is much more than the variation of approximately 20°F experienced with the coverall on. The variation of 115°F without the coverall would have been extremely uncomfortable for a man, if not harmful, even for short periods of time. The above comparisons show that a space worker will require more thermal protection than is provided by his pressure suit and environmental control system.

4.1.3 Determination of Heat Transfer

The effectiveness of the thermal protection coverall may be evaluated on the basis of resistance to heat transfer through the garment in simulated space surroundings. A heat balance and several direct approaches were considered for determining the actual heat transfer from the test data.

Solution by a heat balance was the initial approach to determine the heat transfer through the coverall. Measurement of heat absorbed or rejected by pressure suit air flow and by the dummy model would allow a summation for evaluating the total heat transfer from chamber surroundings. A sketch of the heat transfer mechanisms is shown below.

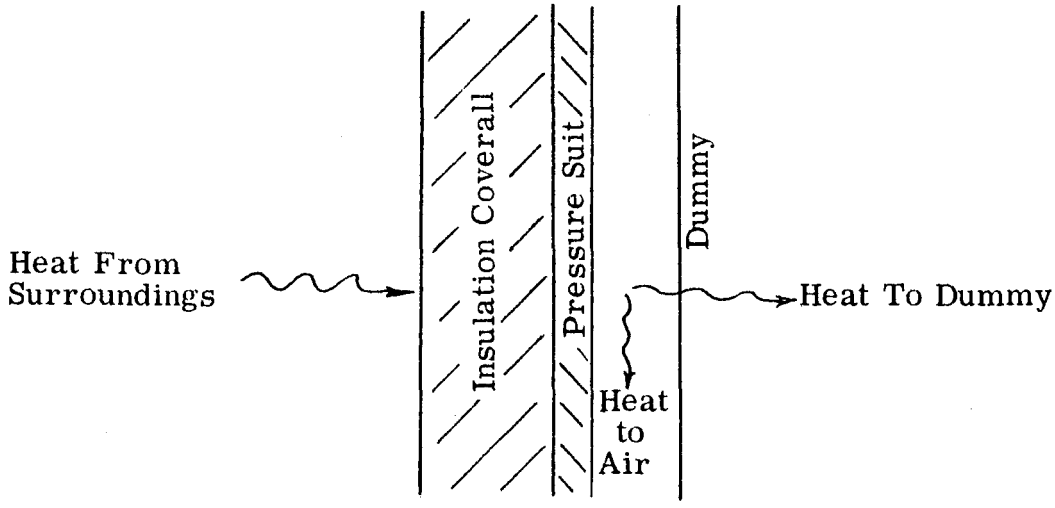

$$Q_{coverall} = Q_{air} + Q_{dummy}$$

Heat absorption or rejection by the pressure suit air flow was obtained from the air mass flow rate and temperature difference between pressure suit inlet and outlet temperatures. The test data showed this temperature difference varied from 0 to 8°F at the steady state test conditions. The values for heat absorbed or rejected calculated from these temperature differences at the steady state test points are shown in Table 9. It should be noted that these heat rates are influenced

[redacted]

TABLE 9

HEAT ABSORBED OR REJECTED BY PRESSURE SUIT AIR

Configuration	Air flow Rate Lb/Min	Air Temperature Change $T_{in} - T_{out}$ ^{o}F	Heat Given up By Air* BTU/Hr	Heat Rate Per Unit Area of suit BTU/Hr-Ft^2
No Sun Coverall on Tinted visor	.250	+6	21.6	0.86
Back to Sun Coverall on Tinted visor	.277	-7.5	-30.0	-1.2
Left side to Sun Coverall on Tinted visor	.282	-7.0	-28.4	-1.1
Front to Sun Coverall on Tinted visor	.282	-8.0	-32.5	-1.3
No Sun Coverall on Clear visor	.273	0	0	0
Front to Sun Coverall on Clear visor	.272	+1	3.9	0.16
Back to Sun Coverall off Clear visor	.273	-4.0	-23.6	-0.94

* Heat given up by air is positive when air temperature is lowered in the pressure suit.

[redacted]

significantly by the dummy conditions and small errors in inlet to outlet temperature difference. The pressure suit air temperature quickly approaches the temperature of the dummy. Therefore, the suit outlet temperature is largely dependent on the surface temperature history of the dummy.

The second step necessary for the heat balance approach was determination of the heat absorbed or rejected by the dummy. This determination was a problem centered around transient thermal bahavior of the dummy bulk. For instance, the dummy may be considered an isothermal body at the start of a typical testing sequence. Then as the chamber is cooled down, a changing dummy surface temperature will set up a gradient at the surface of the dummy material. This gradient determines the heat flow to or from the dummy bulk. As the surface temperature change diffuses through the dummy material the thermal gradient at the dummy surface and corresponding heat transfer continually change.

During the test program the dummy surface temperature was surveyed at three locations, the bridge of the nose, the left finger tip and the left front thigh. Only the left front thigh temperature could be considered a candidate for typical dummy surface behavior. The bridge of the nose was not protected by the thermal insulation coverall, and as the temperature profiles (Figures 17 to 23) clearly indicate, the left finger tip temperature varied considerably more than the dummy surface temperatures obtainable from other profiles which could be extrapolated through to the dummy surface.

An estimate of the dummy heat transfer requires detailed study of the time temperature history of the entire dummy surface up to the point where the data for a heat balance is required. Assuming numerous dummy surface temperatures are available, the problem does not become distinctly unmanageable until tests wherein the solar source is incident on only one side of the model are encountered. Under such conditions a thigh bulk, chest section, or forearm mass would experience reverse gradients from back to front depending of course on what the time temperature history of a particular location is beforehand.

The following approach was undertaken to determine the heat rejected by the dummy in the cold chamber tests (no solar heating). First the thigh temperature time history of the dummy surface was assumed to be applicable to the solarplexus front or back regions where no data was available. The time-temperature history of the dummy surface up to the steady state test point showed an increase of 10°F over about 2 hours of test time.

The second assumption was that of one dimensional heat conduction into a semi-infinite rubber wall. This assumption neglects the change of material from vinyl outer layer to foam rubber inner structure and further neglects the effect of the internal aluminum support structure.

Using a thermal diffusivity of .00024 ft^2/hr. A Schmidt plot analysis was made for the dummy. The surface temperature change as a function of time was accounted for. The results of this analysis are shown in Figure 24. Because of the low thermal diffusivity of the material, the surface gradient is slow to dissipate. Furthermore, the surface gradient is continually reinforced as the surface temperature changes with time.. Calculating the rate of heat transfer from the surface temperature gradient indicates the dummy is rejecting heat at about 8.9 BTU/hr ft^2. Because of the large heat capacity of the dummy, this heat rate is much higher than the heat rejected from the airflow at the same conditions as shown in Table 9.

The thermal gradient from the Schmidt plot and the resulting rate of heat transfer are very sensitive to just one or two degrees of error in surface temperature. For this reason and because the thigh gradient may not be typical for all other dummy areas, the transient analysis for the dummy heat absorption and rejection was not pursued further either by closed form solutions or detailed finite difference methods.

As shown in the above discussions of heat absorption or rejection by the dummy and the pressure suit air flow, the net heat transfer to or from the chamber surroundings through the insulation garment could not be accurately deduced by a heat balance approach.

Several other more direct approaches using test temperature data were considered. In a cold chamber condition the outer surface of the coverall approximates behavior of a surface radiating to a black body at -310°F (chamber cryogenic wall temperature). The outer surface temperature is, then, a direct function of the heat transfer through the coverall garment and the surface emissivity. Figure 25 shows heat transferred through the coverall as a function of surface temperature for emissivities of 0.1 to 0.7. The outside coverall temperatures at cold chamber test conditions varied from approximately -100°F to -200°F (Figures 17 and 18). Although good emissivity data on aluminized mylar was not available at the writing of this report, an emissivity of 0.5 was estimated. This is the value for a 1/4 mil. coating of lacquer on polished aluminum as determined by a comparison of references 3 and 4. Considering a surface emissivity for the mylar coating of 0.4 to 0.6 the heat transfer is between 3 and 10 BTU/hr ft2.

An additional heat transfer estimate was made by assuming an apparent thermal conductivity of the multi-layer insulation and using test results for the temperature difference across the insulator. Figure 26 shows the heat transfer for apparent thermal conductivity from .0001 BTU/hr ft°F to .0015 BTU/hr ft°F.

The apparent thermal conductivities of multi-layer insulation materials depend on the temperatures on either side of the insulation, the technique used in multi-layer buildup, and the pressure between the material layers.

By assuming an apparent conductivity, the heat transfer may

FIGURE 24

DUMMY GRADIENT AT SURFACE

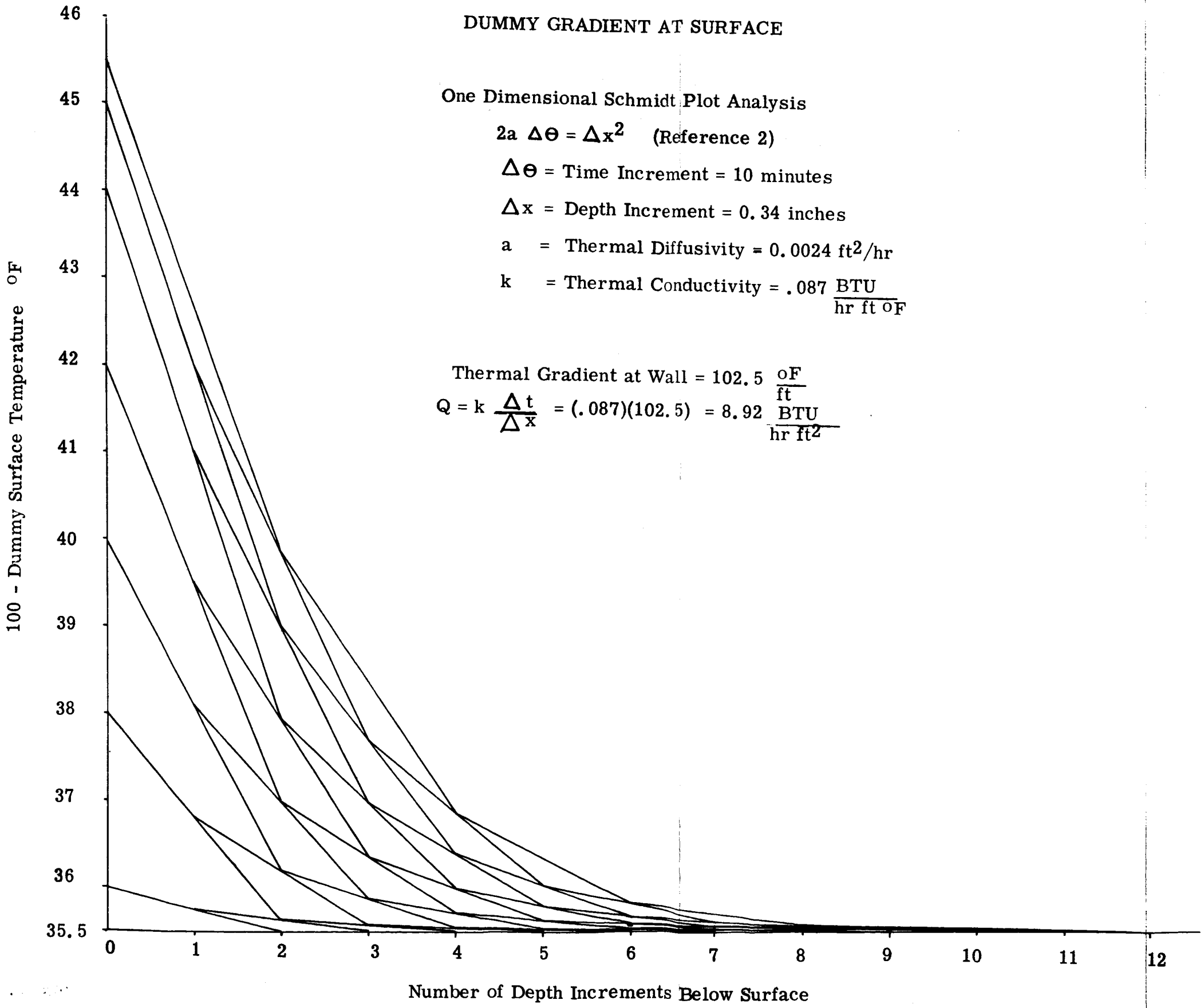

One Dimensional Schmidt Plot Analysis

$2a\ \Delta\Theta = \Delta x^2$ (Reference 2)

$\Delta\Theta$ = Time Increment = 10 minutes

Δx = Depth Increment = 0.34 inches

a = Thermal Diffusivity = 0.0024 ft^2/hr

k = Thermal Conductivity = .087 $\frac{BTU}{hr\ ft\ ^oF}$

Thermal Gradient at Wall = 102.5 $\frac{^oF}{ft}$

$Q = k \frac{\Delta t}{\Delta x} = (.087)(102.5) = 8.92 \frac{BTU}{hr\ ft^2}$

FIGURE 25

HEAT TRANSFER TO COLD CHAMBER
SURROUNDINGS BASED ON SURFACE EMISSIVITY

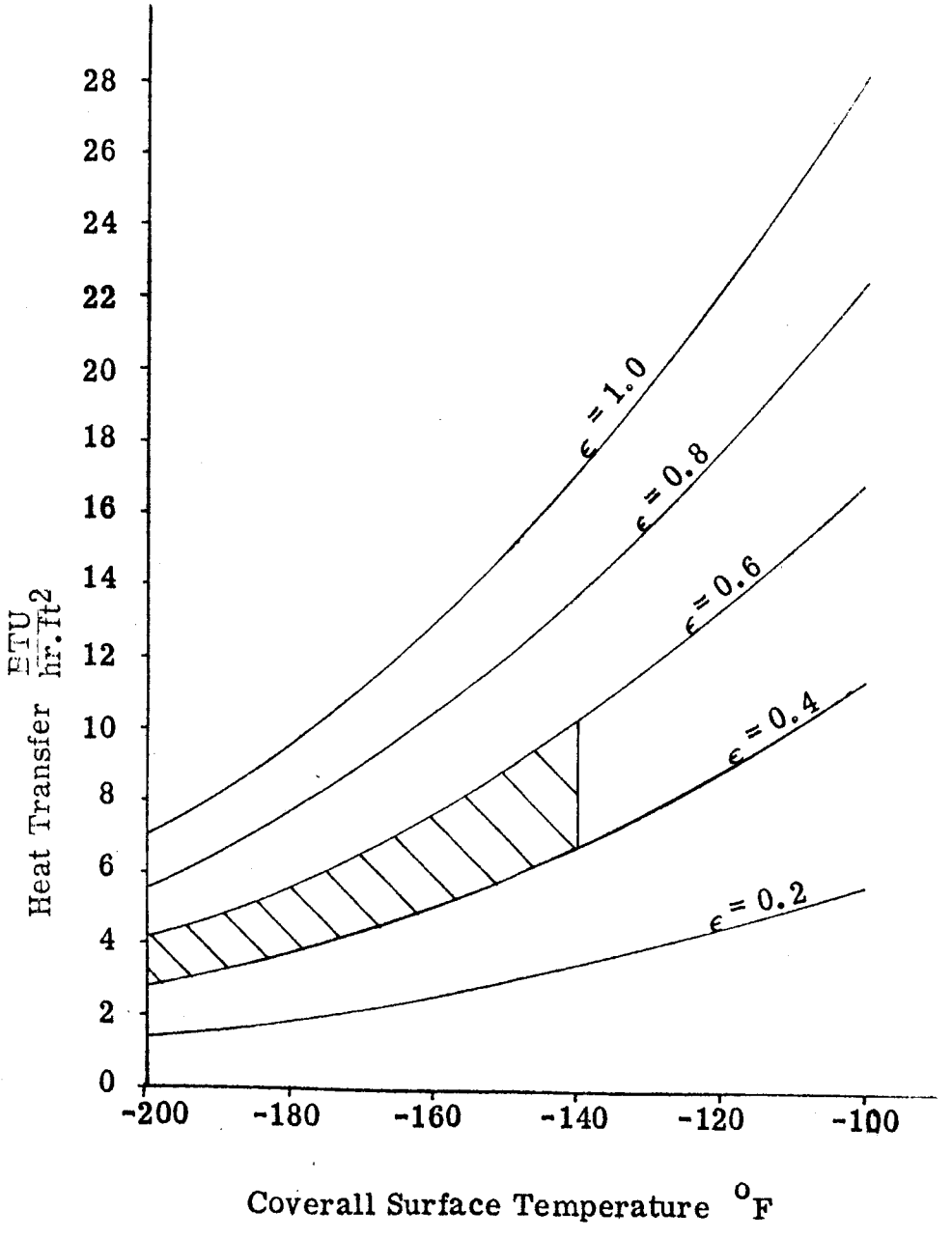

FIGURE 26

HEAT TRANSFER TO COLD CHAMBER SURROUNDINGS
BASED ON APPARENT CONDUCTIVITY OF MULTI-LAYER INSULATION

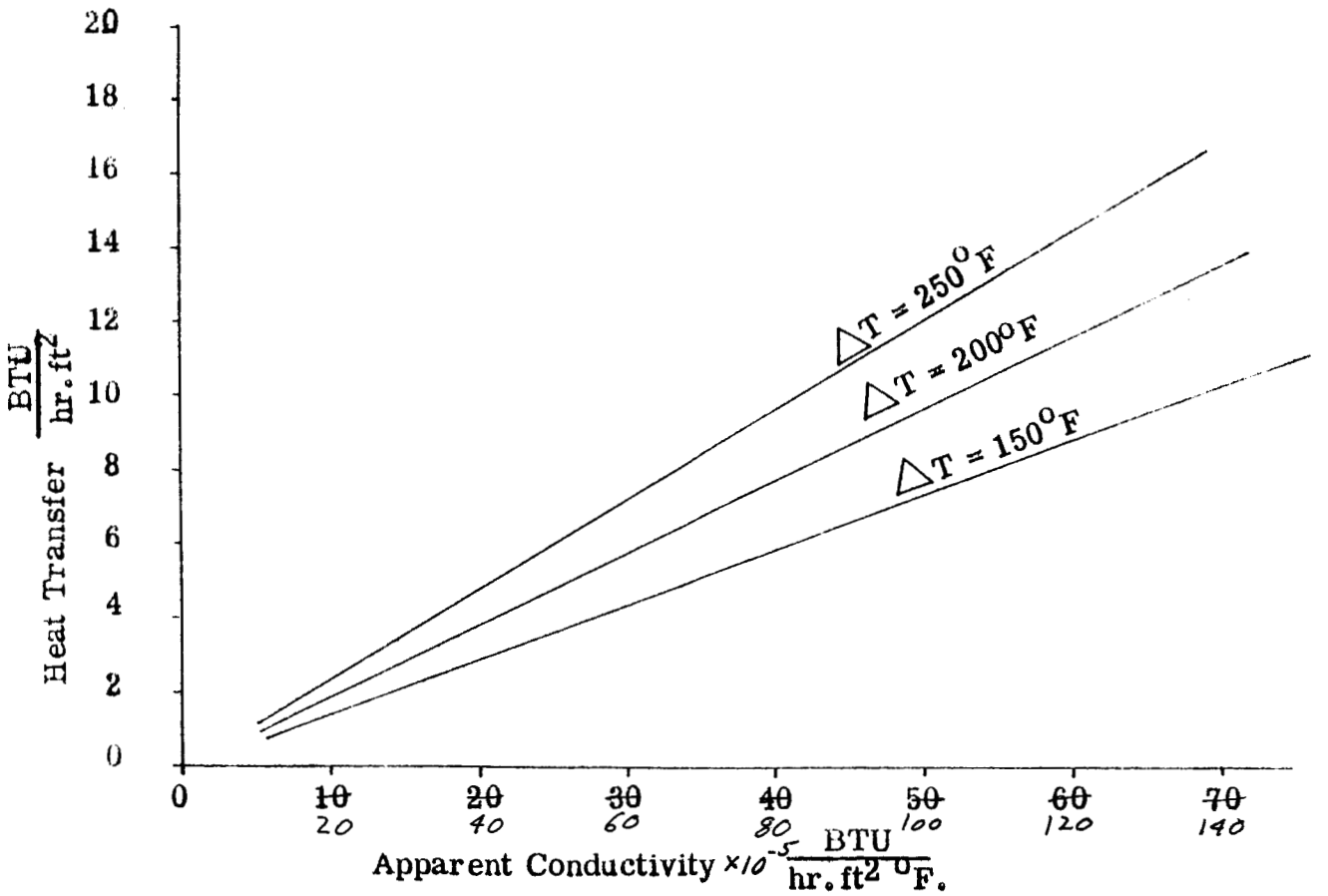

be bracketed for any test condition. At cold chamber conditions, a conductivity of .00025 to .00135 is required for the heat transfer to match the previous value of 3 to 10 BTU/ hr ft^2 calculated on surface emissivity basis in cold chamber surroundings. This thermal conductivity appears somewhat high but is a reasonable number.

Accurate analysis of the heat transfered through the insulated coverall was impossible due to the large heat capacity of the dummy and the uncertainty in its temperature history. By approaching the heat transfer problem from the coverall temperature data, however, the rate of heat transfer through the coverall was bracketed between 3 and 10 BTU/hr ft^2 in the simulated cold space environment. The rate of heat transfer may be defined even further when better data on the emissivity of the aluminized mylar (mylar side) and/or thermal conductivity at test conditions become available.

4.1.4 Garment Deterioration

After two days of testing, deterioration of the outer layer of the coverall garment was evident, and after three days of testing, the deterioration was quite severe. The coverall material was examined closely to determine the nature of the deterioration.

The thin mylar layers of the multi-layer thermal protection garment were aluminized on only one side. An ohm meter was used to measure outside coverall surface resistivity after the tests were run, thereby giving an indication of whether aluminum or mylar faced the chamber surroundings. Nearly all surfaces of the coverall had mylar facing the space environment, the exceptions being the left hand mitten and a 2" wide strip on the back of the helmet.

As the tests progressed the outermost layer of aluminized mylar on the insulated garment showed extensive deterioration. This outside layer pulled apart at the slightest touch or under the force of its own surface stress. Figures 27 and 28 show coverall damage after the second and third day of testing, respectively.

Surfaces on which the aluminum coating faced the chamber surroundings showed considerably less deterioration than the surfaces on which the mylar faced the chamber environment. Figure 29 shows a comparison of the two hand mittens. The mitten on the left side had the aluminum surface facing outward. Both mittens had been exposed to the space environment for a total of approximately 23 hours.

The yellowing of the surfaces on which mylar faced the chamber surroundings would seem to indicate a detrimental ultraviolet effect. The aluminized surfaces which faced the solar source would be expected to get hotter. Yet the deterioration by increased temperature and vacuum did not seem to cause as much breakdown as when mylar faced the simulated space environment. This also indicates a detrimental effect due to ultraviolet light.

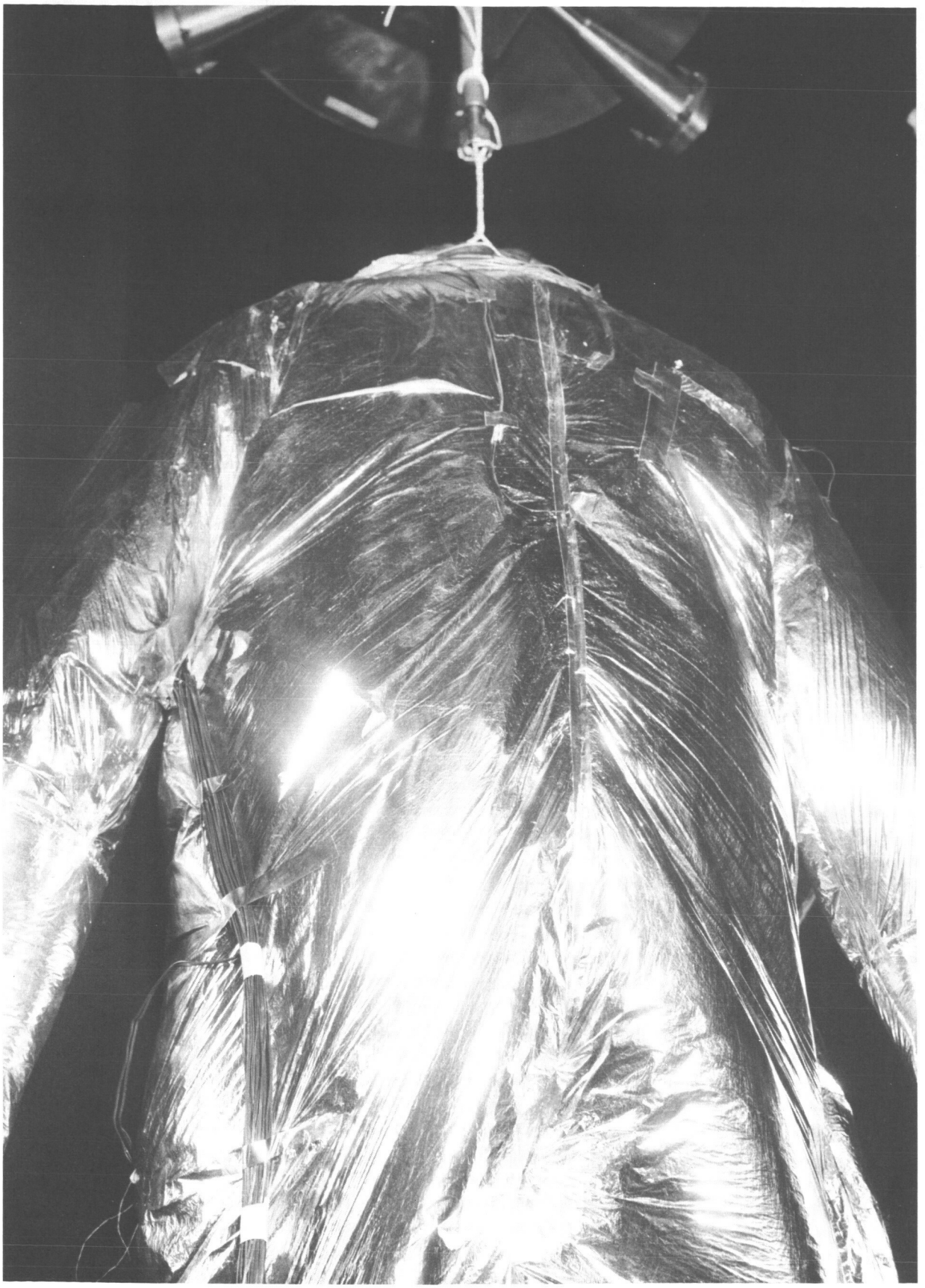

Figure 27 COVERALL DETERIORATION AFTER 2ND DAY OF TESTING

Figure 28 COVERALL DETERIORATION AFTER 3RD DAY OF TESTING

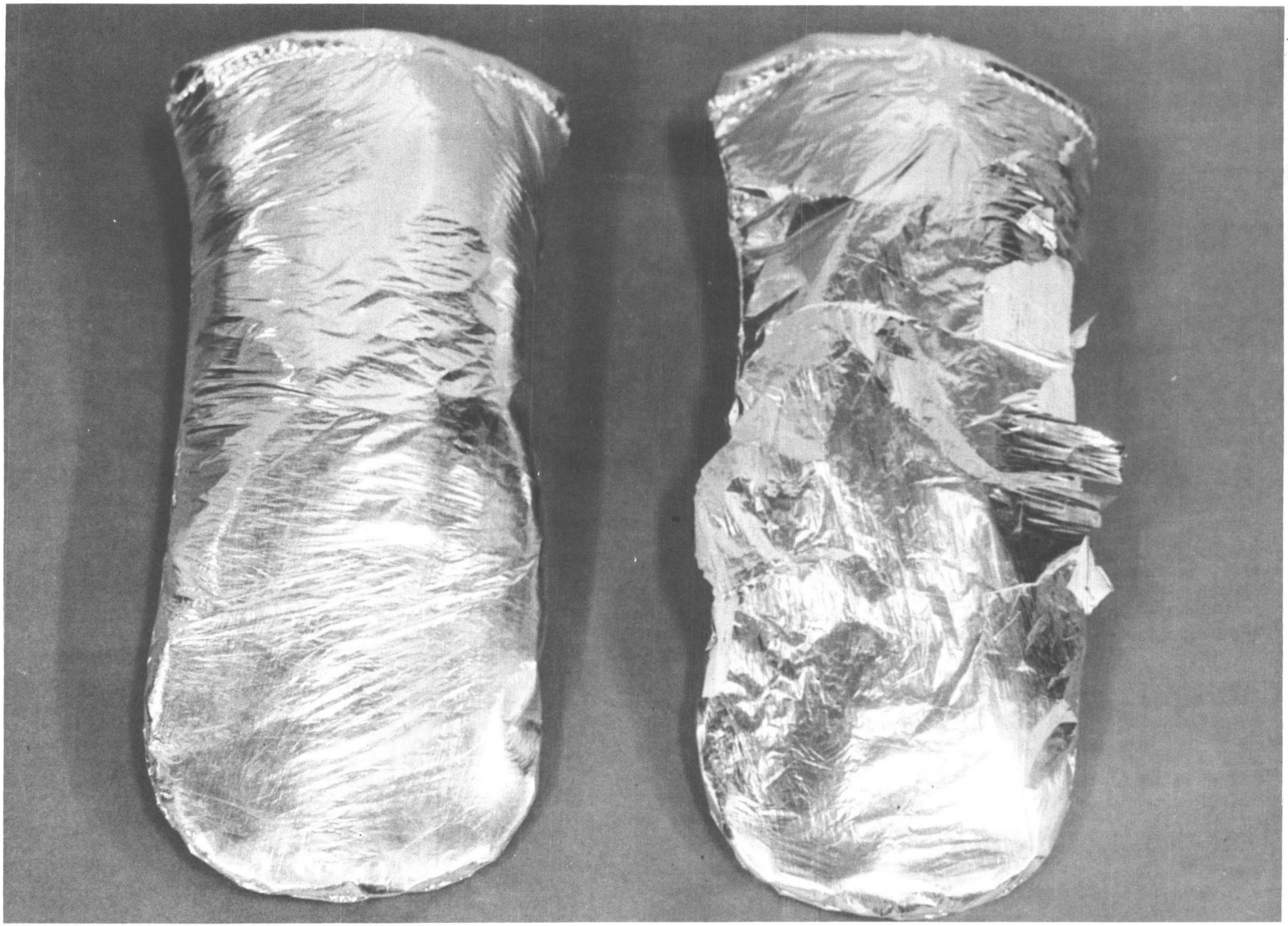

Figure 29 COMPARISON OF MITTEN DETERIORATION

[redacted]

The closeness of the outside coverall temperatures at the cold chamber condition on the 1st and 3rd day indicates no significant change in surface emissivity took place between these test runs.

4.2 Visor Shield Performance

4.2.1 Temperature

The performance of the gold tinted visor shield can be evaluated by comparing the dummy and visor temperatures with and without the visor shield. The temperatures of the dummy, visor, and visor shield are summarized in Table 10 for the seven steady state test points.

When the visor is exposed to the cold space environment, heat is radiated to space and the visor is cooled. The temperatures in Table 10 for configurations 1 and 2 indicate that the visor temperature was 26°F without the shield as compared to 51°F with the shield in place. The dummy temperature does not appear to have been affected, however. The temperatures in the test of configuration 6 verifies the cold environment visor temperatures of configuration 2.

Immediately after the test of configuration 6, the test article was turned to face the sun (100 minutes-Figure 16). It was observed that moisture from the air in the pressure suit had condensed and frozen on the visor. This is shown in Figure 30a. After a few minutes of exposure to solar heating the frost dissipated. The test article is shown on Figure 30b after the frost had dissipated. The frost would have completely blocked vision and indicates the requirement for the visor shield or some other means of controlling the visor temperature. As shown by the test results for configuration 1 and 5 (Table 10) the tinted visor shield maintained the clear visor temperature very near the temperature of the dummy and no condensation or freezing was observed.

The visor shield appeared to have negligible effect on the dummy and visor temperatures when the front of the dummy was illuminated by the sun. The visor and dummy temperatures obtained from the tests of configurations 3 and 4, Table 10, are essentially the same. The differences may be attributed to previous history of the dummy temperature.

Thermal response of the visor and visor shield to changes in environmental conditions during the 2nd day of testing are shown by the transient curves of Figure 31. After a step change in environmental conditions, both temperatures appear to approach steady state values in about 1-1/2 hours. As was expected, the variation of the inner visor temperature was much less than the variation in visor shield temperature.

[redacted]

TABLE 10

VISOR TEMPERATURE SURVEY AT STEADY STATE

Configuration		Coverall	Colored Visor Shield	Temperature °F		
				Inside Visor Shield	Inside Clear Visor	Bridge of Nose
1.	No Sun	On	On	46	51	55
2.	No Sun	On	Off	~	26	56
3.	Front Facing Sun	On	On	172	101	103
4.	Front Facing Sun	On	Off	~	100	109
5.	Back Facing Sun	On	On	56	66	66
6.	Back Facing Sun	Off	Off	~	26	50
7.	Left Side Facing Sun	On	On	86	76	78

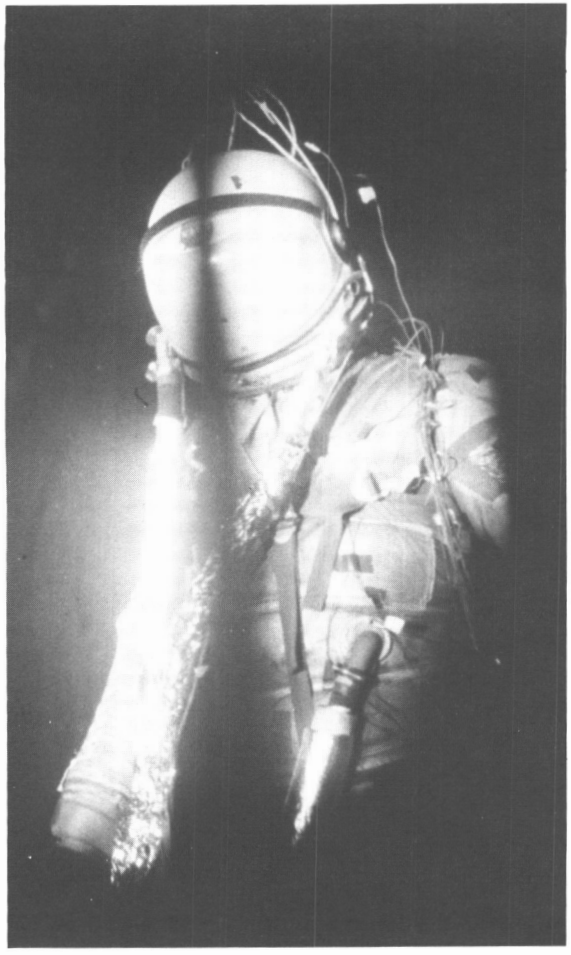

Figure 30a

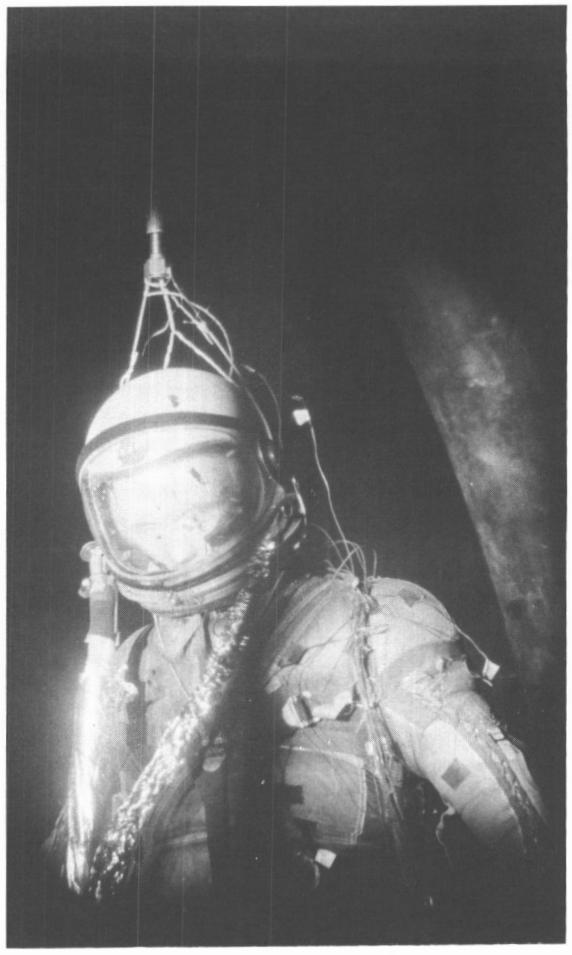

Figure 30b

VISOR FROSTING

FIGURE 31

VISOR AND VISOR SHIELD THERMAL BEHAVIOR DURING 2ND DAY OF TESTING

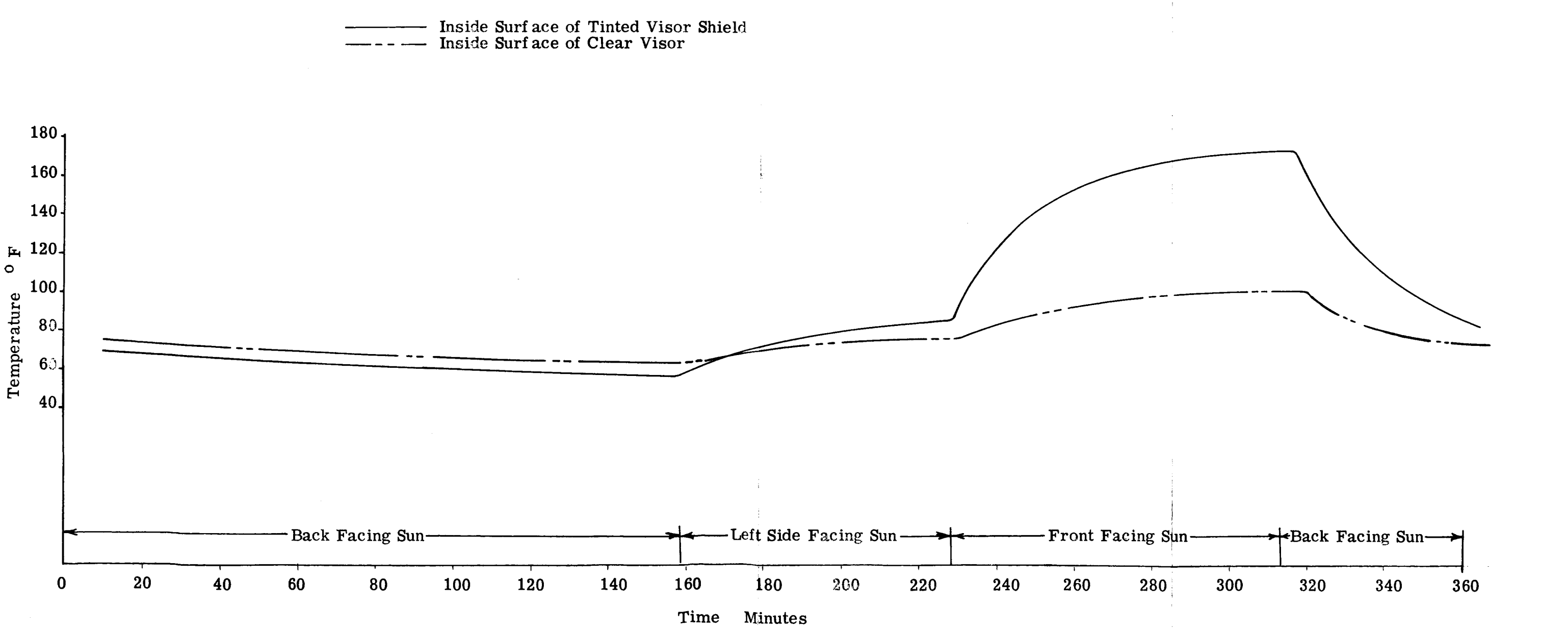

[redacted]

4.2.2 Visor Deterioration

Both the visor and visor shield showed signs of deterioration after testing. A picture of the visor shield after being used in the tests is shown in Figure 32. Deformation of the shield and irregularities (peeling, flaking and bubble formation) in the gold film are evident at the upper part of the shield. This part of the surface was perpendicular to the solar rays during tests with the front of the test article facing the sun. Maximum temperatures recorded near the center of the visor shield were approximately 170°F. The temperatures in the area of deformation could have been somewhat higher because of the curvature of the surface. There was no instrumentation in the exact area of deformation.

When the damaged visor shield was removed, the clear visor showed no signs of deterioration. After exposure to space environmental conditions during the rest of the tests, the clear visor had also deformed. The space suit helmet and clear visor are shown in Figure 33 after tests. The arrow indicates visor deformation evident after testing. Before testing, the visor had a smooth curved surface. Maximum clear visor temperature recorded near the center of the visor was approximately 100°F.

The clear visor serves as a pressure shell and the pressure inside was always significantly higher (3.0 to 3.5 psi) than the chamber pressure during the tests. If the deformation were due to heating and softening of the visor, the deformation could be expected to go outward. As may be seen in Figure 33, however, the deformation was inward. A possible explanation is that the deformation is caused by polymerization and changes in the visor material due to ultraviolet light. The outer surface would be attacked more severely, possibly causing shrinkage of the outer layer. This could account for the inward deflection of the visor material.

[redacted]

Figure 32 VISOR SHIELD DETERIORATION

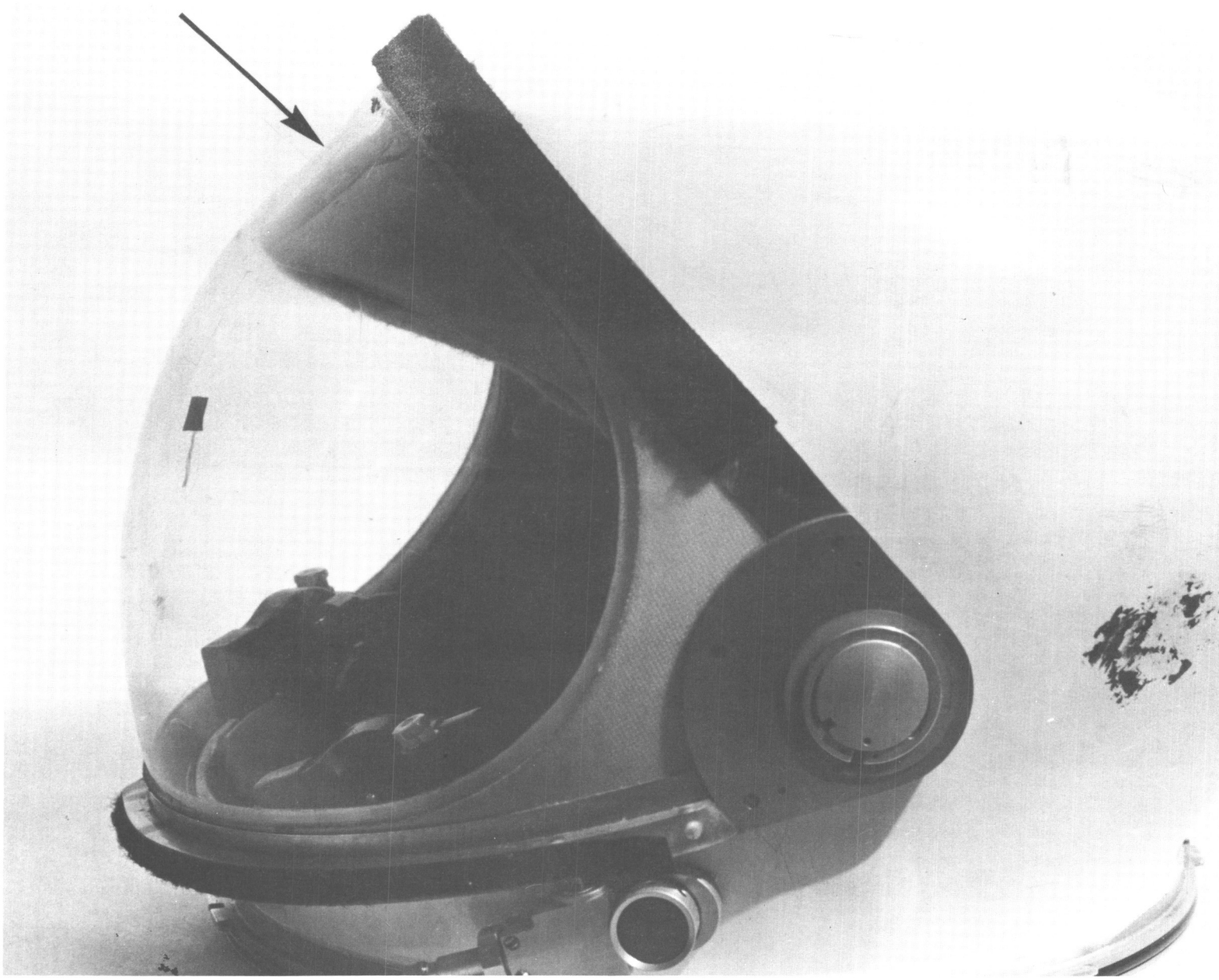

Figure 33 CLEAR VISOR DETERIORATION

5.0 CONCLUSIONS

The objectives of this test program were accomplished. These were the determination of the feasibility and effectiveness of the insulated coverall garment concept for extravehicular space suit thermal control. Feasibility of using the coverall was demonstrated by its ability to control temperatures of the dummy and the air surrounding the dummy to comfortable limits while the outer surface experienced variations between -200° F. and +240° F. The thermal control provided by the coverall garment was adequate for all orientations and environmental conditions tested.

The thermal effectiveness of the coverall was demonstrated by the large temperature differences between the inner and outer layers of the coverall material and by heat transfer estimates based on coverall temperatures. Temperature differences on the order of 200° F occurred across the coverall while the temperature difference across the pressure suit at the same time and location was less than 5° F. This indicates that the thermal resistance of the coverall was at least 40 times the resistance of the suit only. Because of the errors introduced by the large heat capacity of the dummy, an accurate heat balance of the coverall garment was not possible. Other approaches based on coverall temperatures were used, however, to bracket the heat transferred through the garment to a cold environment (no solar heating) between 3 and 10 BTU/hr ft^2.

The gold coated visor shield provided enough thermal protection for the pressure suit helmet visor to prevent moisture condensation and freezing in the cold environment. Under these conditions, the difference in pressure suit helmet visor temperature and dummy temperature was not more than 4° F. When the solar heating was directed at the face of the visor, however, the visor shield appeared to have no appreciable effect on dummy or helmet visor temperatures.

Sufficient elemental tests should be performed on the selected materials and coverall construction to verify the selected design. After the coverall has been modified to meet the optimum insulation and material requirements, a full size garment should be tested in a simulated space environment. This test would be similar to those performed in this test program. A light, thermally thin dummy should be used so that more accurate heat balance data can be obtained. A movable dummy might be desirable to study the effects on heat transfer of flexing the joints.

6.0 RECOMMENDATIONS

Based on the results of this test program, several areas in which additional study should be undertaken have been defined. They are briefly outlined below:

1) The radiative surface properties of the coverall garment and the insulation thickness should be optimized for the worst anticipated environmental conditions. In a cold environmental (no solar heating, no radiation from planets, etc.) the heat losses from the coverall depend primarily on the conductivity and thickness of insulation as well as the emissivity of the outer surface. When the coverall is illuminated by the sun and/or receives radiation from the lunar surface, the heat transfer is dependant on the solar absorptivity of the surface in addition to the emissivity of the surface, conductivity of insulation, and insulation thickness. An ideal surface would be one that had a low emissivity and a low ratio of solar absorptivity to emissivity.

2) A suitable outer covering for the coverall would be one that has the desired radiative properties, flexibility, strength, and resistance to deterioration in the space environment. The radiative properties of the outer surface should be optimized by considerations such as those described in the previous paragraph. Selection of the proper material will involve a screening of candidate materials and testing to determine detrimental effects of ultraviolet radiation, vacuum, and temperature.

3) Materials for the helmet visor and visor shield that do not deteriorate in the space environment are required. Although the gold coated visor shield appeared to offer adequate protection in the cold environment, some means should be devised to limit the apparent brilliance of the sun as a crewman faces it.

LIST OF REFERENCES

1. Hansen, Robert, et. al., "Annotated Bibliography of Applied Physical Anthropology in Human Engineering," WADC TR 56-30, May 1958.

2. Kreith, Frank, Principles of Heat Transfer, International Textbook Company, Scranton, 1958.

3. Moore, Louise, et. al., "Evaluation of the Mechanisms which Affect the Performance of Thermal Radiation Resistant Coatings," WADC Technical Report 57-334, Armour Research Foundation, Chicago, 1957.

4. Gubareff, J. E., et. al., Thermal Radiation Properties Survey, Second Edition, Honeywell Research Center, Minneapolis-Honeywell Regulator Company, Minneapolis, 1960.